MICRO Imaging of the Brain's Microvasculature

Sagar Buch, Ph.D.

Department of Radiology
Wayne State University



Vascular Imaging

- Imaging the microvasculature is key to unlocking the etiology of many neurodegenerative diseases including: dementia, hypertension, multiple sclerosis, Parkinson's disease, stroke, and traumatic brain injury (TBI)
- It is difficult to detect small vessels ($<250\mu$) using conventional MRI due to the lack of contrast and/or imaging resolution

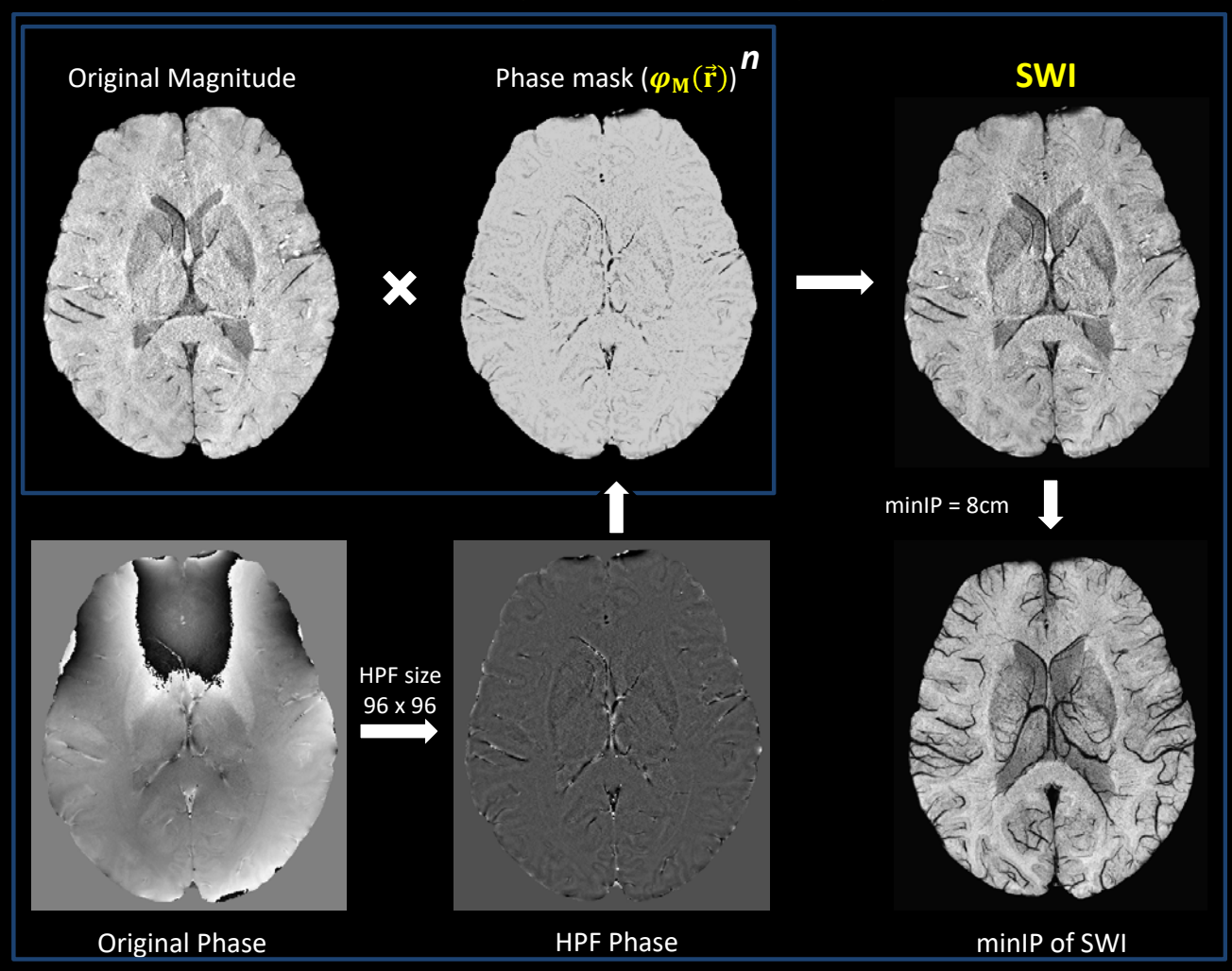
Microvascular In-vivo Contrast Revealed Origins: MICRO

- MICRO enables superior microvasculature imaging by:
 - 1. Using ultra-small superparamagnetic iron oxides (**USPIO**) to induce an increase in susceptibility in both *arteries and veins*
 - 2. Employing high spatial resolution to increase small vessel visibility
 - 3. Utilizing SWI processing to further enhance the vascular signal loss
- We use low dose *Ferumoxytol*, an FDA approved USPIO agent for treating anemia, to accomplish these goals.

Process of obtaining Susceptibility weighted imaging (SWI) data

$$m{\phi_{M}(\vec{r})} = egin{cases} 1 - rac{|\phi(\vec{r})|}{\pi}, & if - \pi < \phi < 0 \ 1, & else. \end{cases}$$

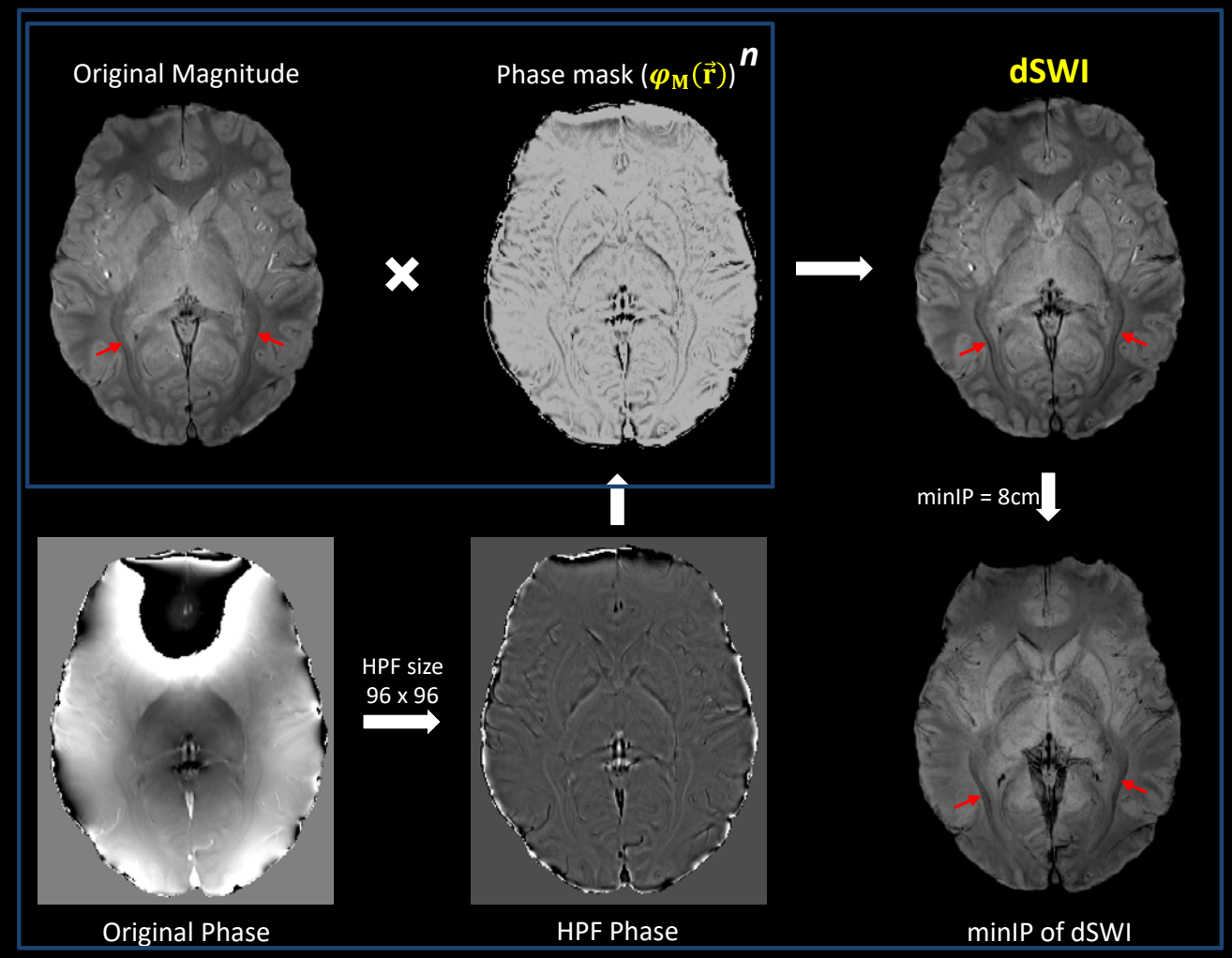
 $\begin{aligned} & \textbf{SWI} = \text{mag} \cdot [\phi_M(\vec{r})]^n \\ & \text{where, n is generally 4} \end{aligned}$



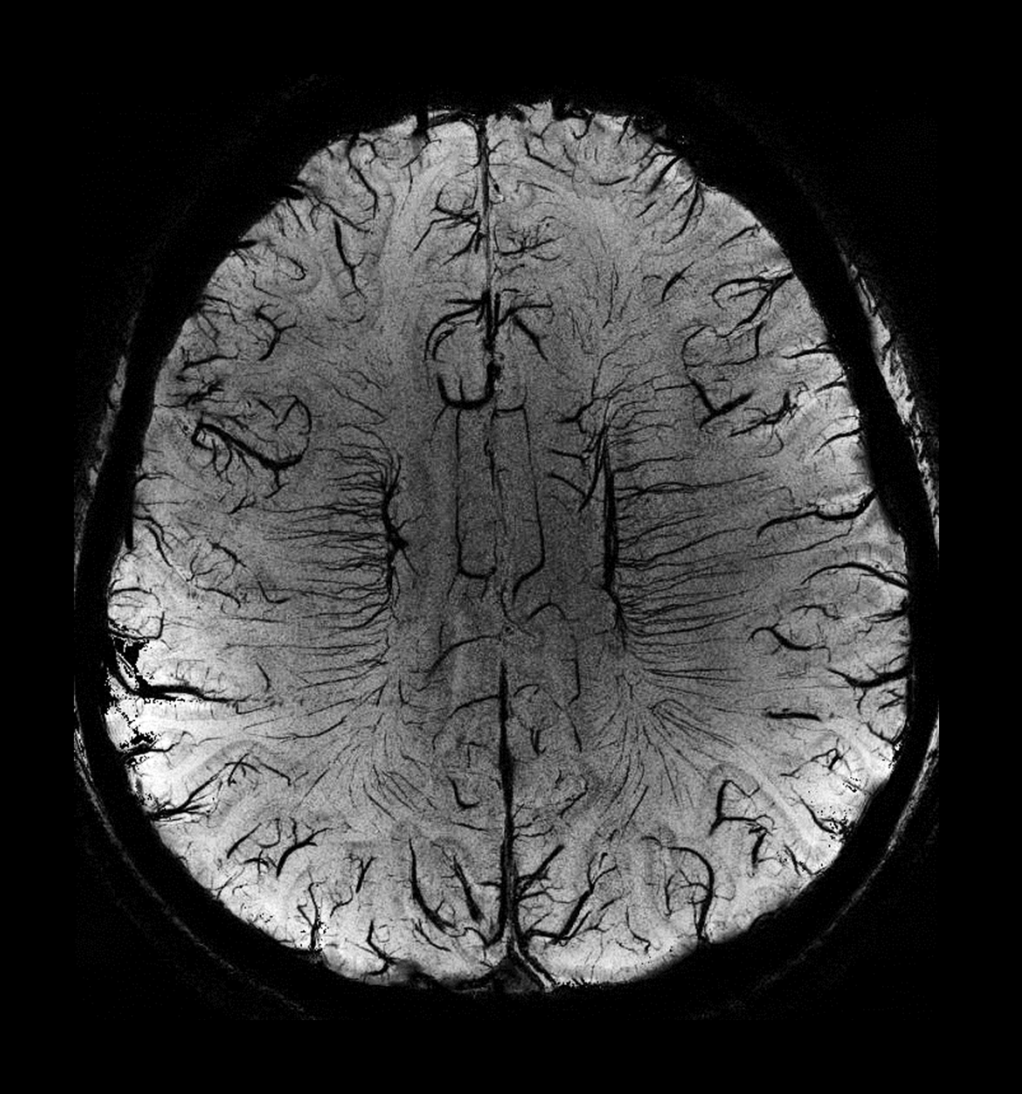
Process of obtaining Susceptibility weighted imaging (SWI) data

$$oldsymbol{arphi}_{\mathbf{M}}(\mathbf{\vec{r}}) = egin{cases} 1 - rac{|oldsymbol{arphi}(\mathbf{r})|}{\pi}, & if & \mathbf{0} < oldsymbol{arphi} < \pi \\ 1, & else. \end{cases}$$

SWI = mag· $[\phi_M(\vec{r})]^n$ where, n is generally 4



Jella, P. K., Y. Chen, W. Tu, S. Makam, S. Beckius, E. Hamtaei, CC-T. Hsu, and E. M. Haacke. "American Journal of Neuroradiology 42, no. 2 (2021): 285-287.



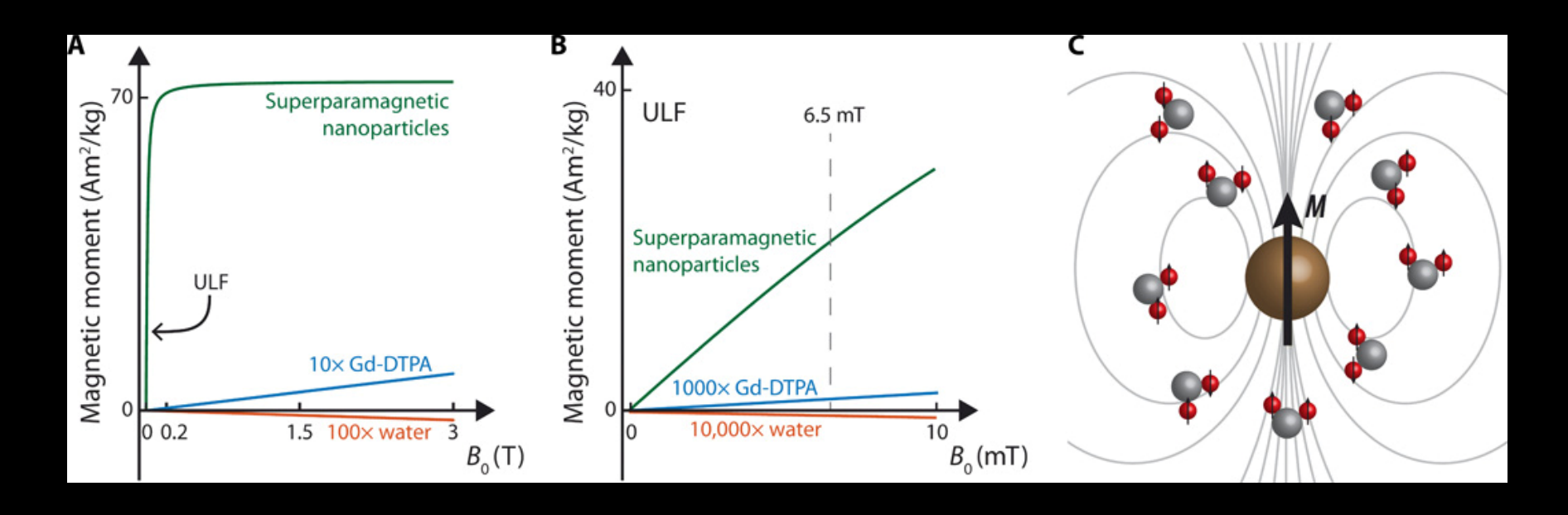
7T SWI non-contrast data

 $215x215x1000\mu m^3$ TE = 16ms, TR = 45ms, FA = 25° 8 slice mIP

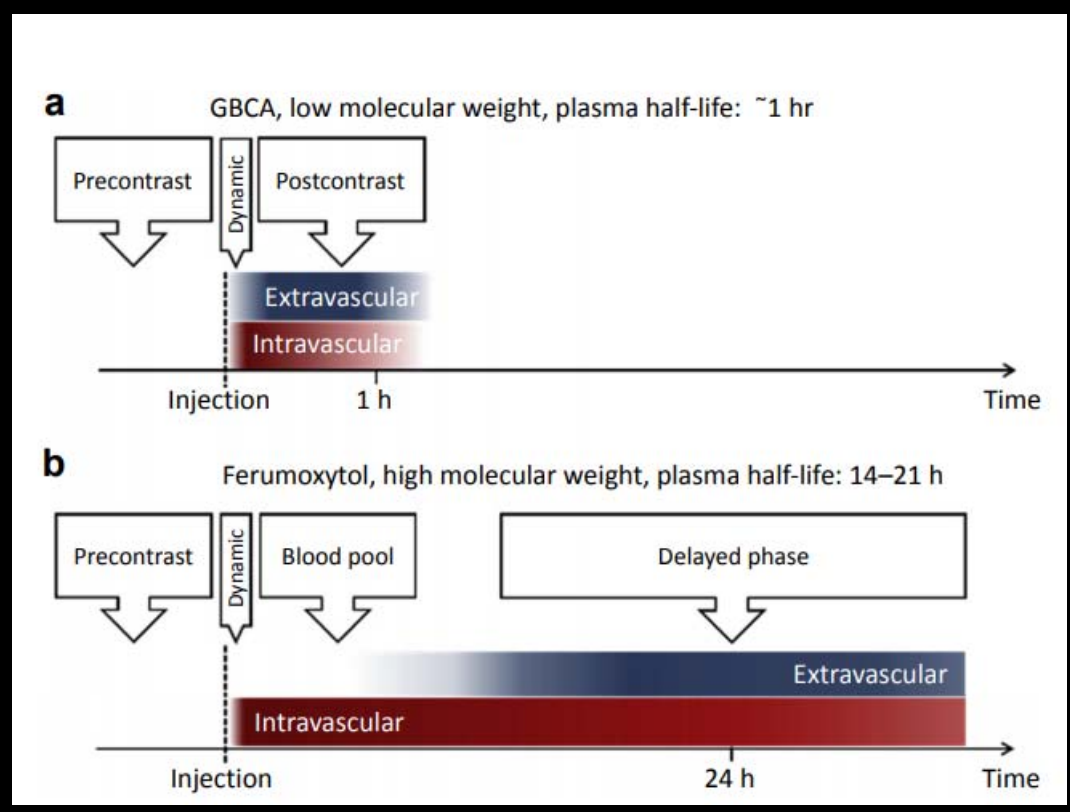
$$\frac{1}{T_{1eff}} = \frac{1}{T_1} + \alpha[c]$$

Feature	Ferumoxytol	Gd-DTPA (Magnevist)
Basic element	Iron oxide	Gadolinium(III)
Molecular composition	Iron oxide coated with semisynthetic	Gadolinium chelated with
	carbohydrate	diethylenetriamine penta-acetic
		acid
Relaxometric properties at 1.5 T/mM per s, 37°C in water	$r_1 = 15, r_2 = 89$	$r_1 = 3.3, r_2 = 3.9^{108}$
Elimination plasma half-life		1.6 h
Relative size of the particle	Approximately 30 nm ¹	0.357 nm
Permeability to intact BBB	Minimal	Minimal
Typical times to peak enhancement (in brain lesions)	24 h ¹¹⁰	3.5–25 min ¹¹¹
Signal change on T1-weighted sequence	Increased signal (signal decreased	Increased signal
	at very high concentrations)	
Signal change on T2-weighted sequence	Decreased signal	Usually no change
Signal change on T2*-weighted sequence	Decreased signal	Decreased signal if given
		as a bolus
Distribution	Dynamic phase, blood pool phase, delayed	Dynamic phase,
	phase (extra and intracellular)	extracellular phase
Imaging dose	1–7 mg/kg	0.1 mmol/kg
Excretion	Stored with the body's iron reserve and used in	Renal
	hemopoesis coating with renal and fecal excretion	
Boxed warning	Potential hypersensitivity	Potential NSF
BBB, blood-brain barrier; Gd-DTPA, gadolinium diethylenetriamine penta-acetic acid; NSF: nephrogenic systemic fibrosis.		

Toth GB et al., Kidney Int. 2017 Jul;92(1):47-66.

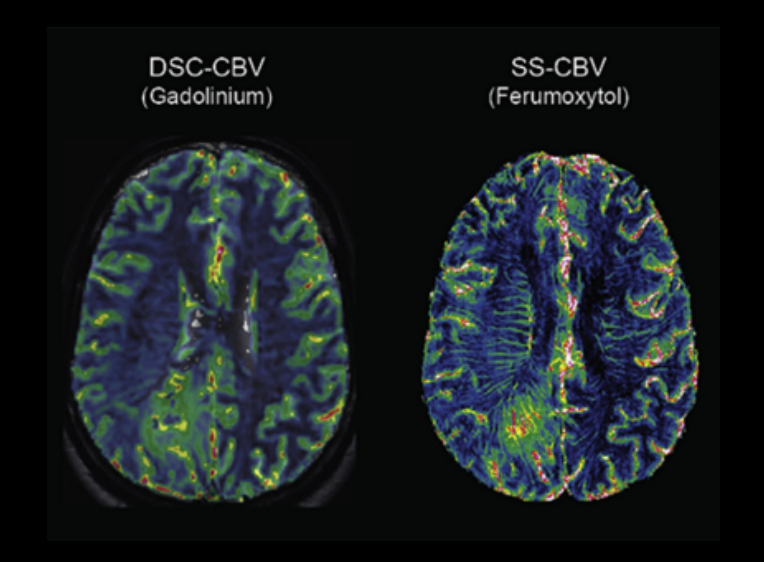


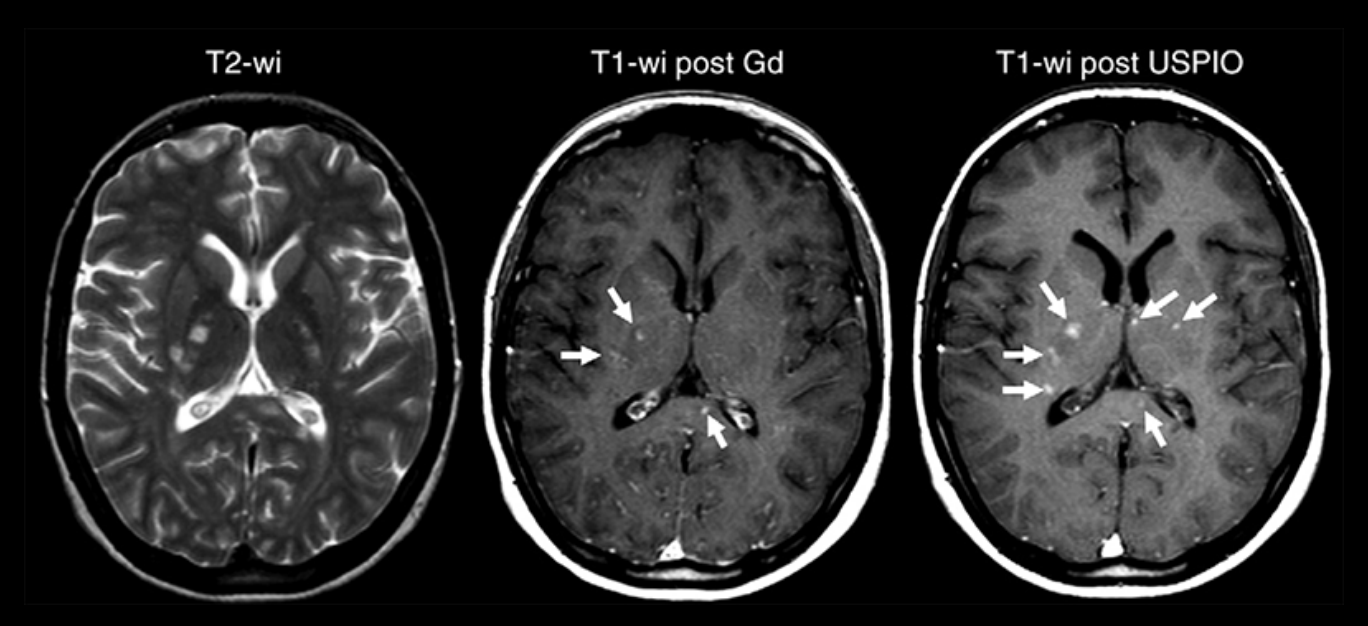
- USPIO is saturated at low fields and so it does not change its properties above roughly 0.5T to 1T.
- USPIOs possess much higher sensitivity than Gadolinium



Toth GB et al., Kidney Int. 2017 Jul;92(1):47-66.

Unlike Gd-based CAs, Ferumoxytol has a long intravascular half-life that results in a *long blood pool phase* prior to detectable contrast extravasation.

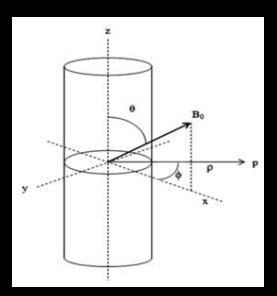




- Ferumoxtran-10 shows the same three lesions along with three additional active lesions that enhanced
- Lesions that enhance with both agents may exhibit a more aggressive evolution than those that enhance with only one contrast agent

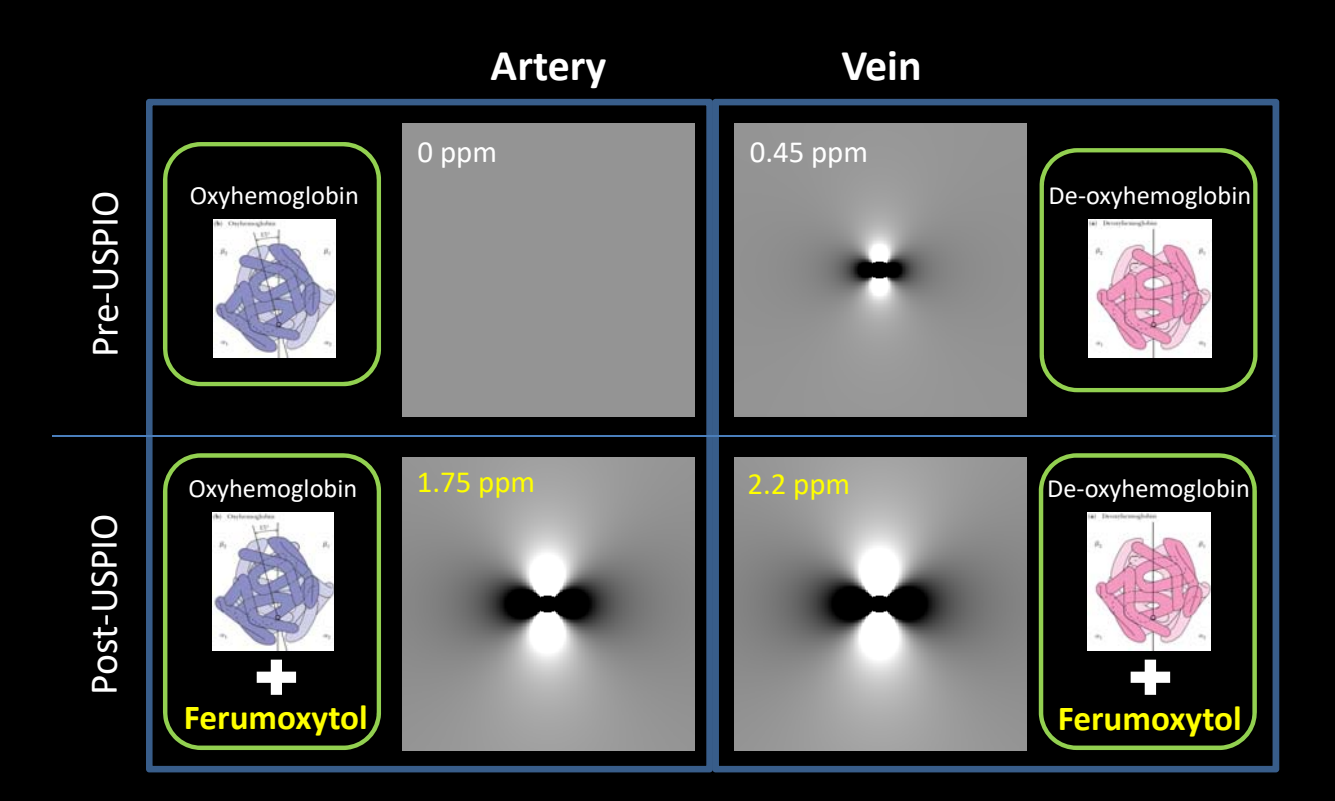
Vascular Phase Behavior

Infinite cylinder model



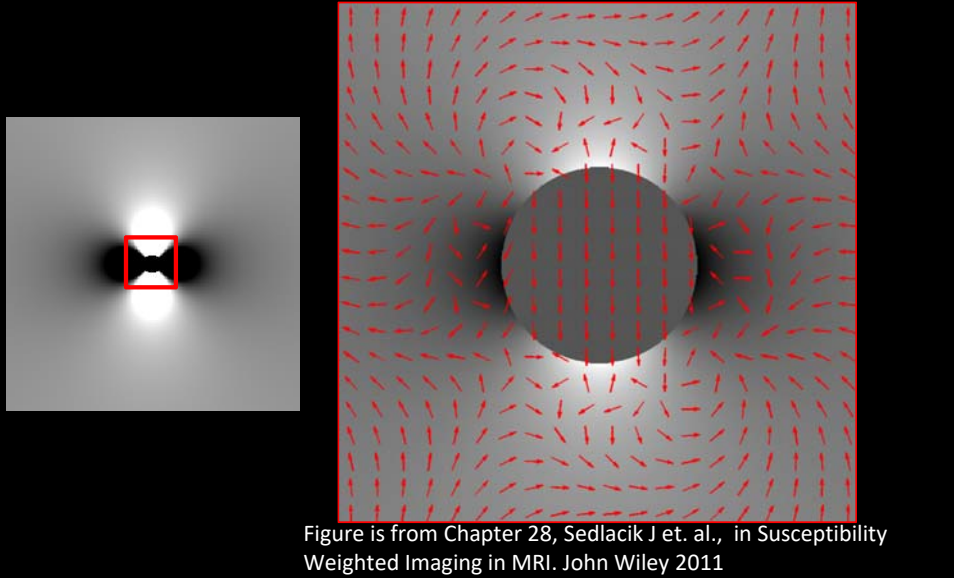
$$\varphi_{\text{External}} = \frac{\Delta \chi}{6} (3 \cos^2 \theta - 1) B_o$$

At Ferumoxytol dose of 4 mg/kg: Δχ increases by 1.75 ppm at 3T



Even with a low Ferumoxytol dose of 4mg/kg, we can induce a strong phase behavior in veins as well as arteries, which were invincible on the pre-contrast SWI phase data

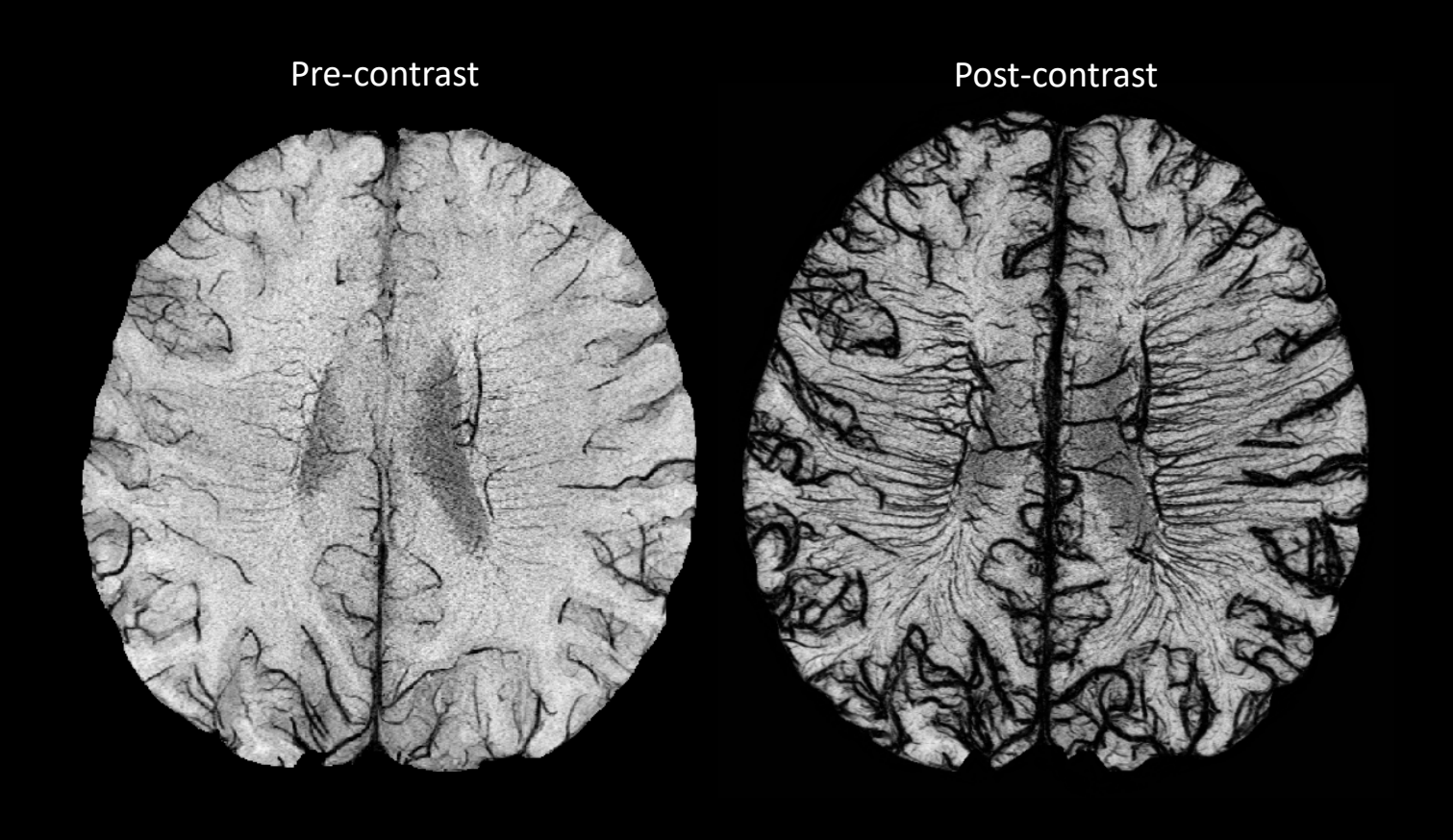
Dipole Phase Behavior Leads to T2* Dephasing





The phase variation that exists outside the vessel or microbleed leads to T₂* dephasing or "the blooming artifact" SWI capitalizes on the phase to further enhance the presence of small veins.

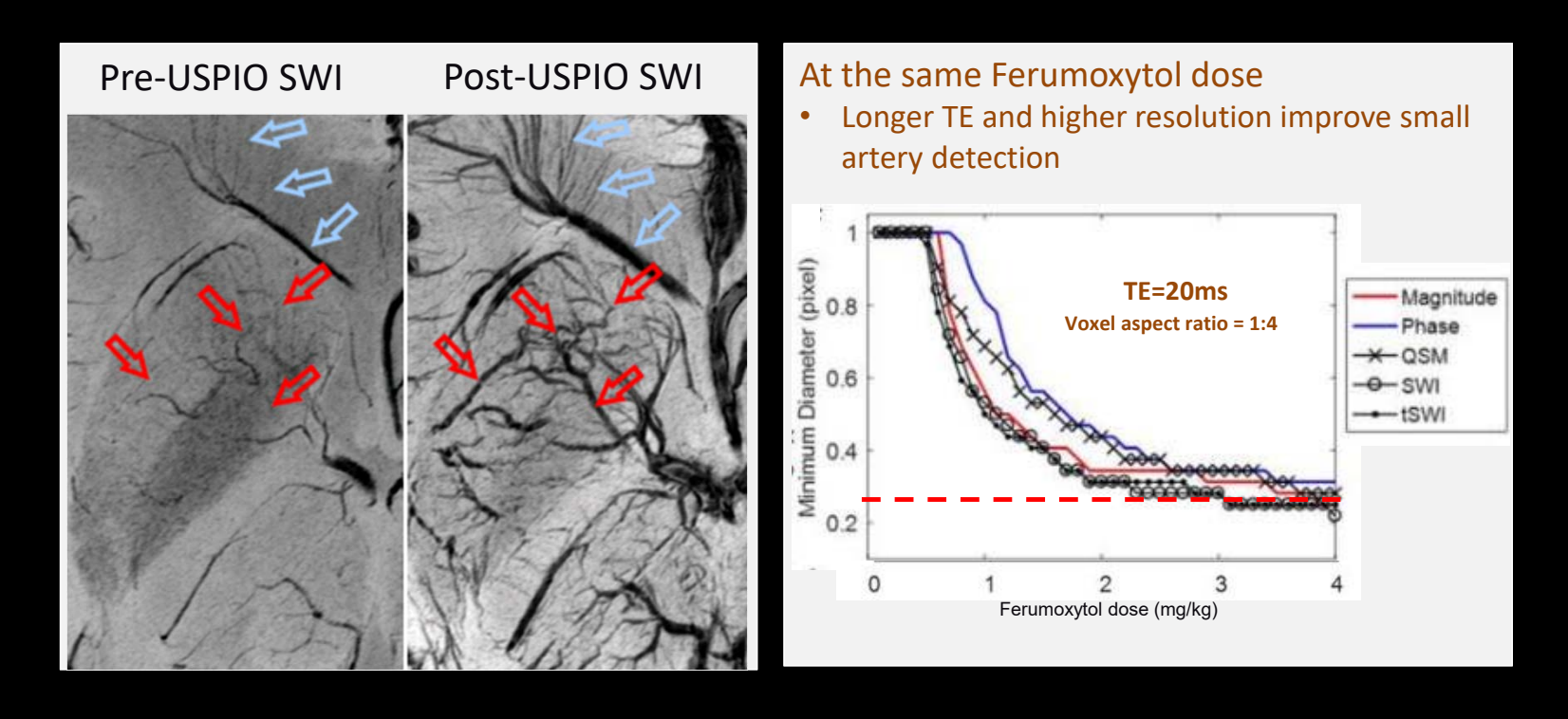
Ferumoxytol enhanced MRAV on 3T



Patient safety

- All subjects with any allergies, low BP, Hemochromatosis or Thalassemia were excluded
- Clinically, it is recommended to administer 7.5 mg/kg in patients who are anemic, over at least 15 min period along with saline
- The maximum dose does not exceed <u>4 mg/kg</u> along with 50ml of saline, which was administered over 20 mins
- All subjects were monitored for 30 min after administering Ferumoxytol
- A trained nurse or Physician is always required to be present during the study at the MR scanner
- To date more than 60 subjects have been scanned without any effects

What is the smallest vessel we can see with MICRO?

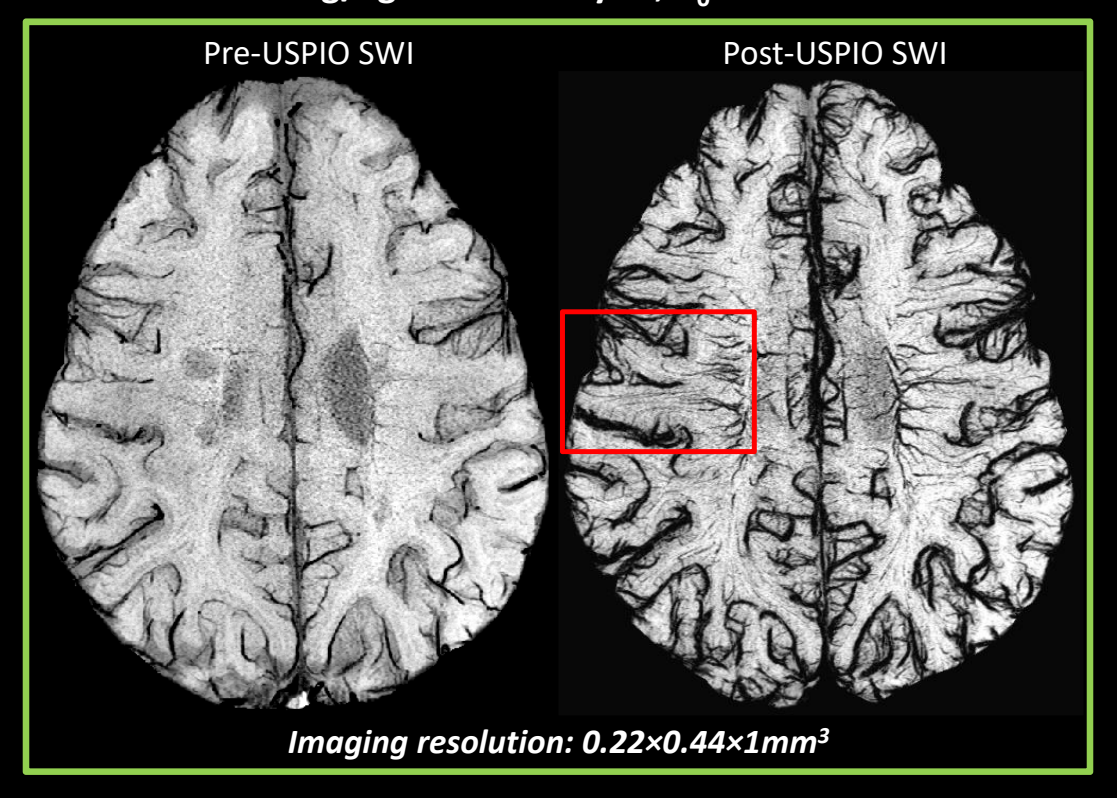


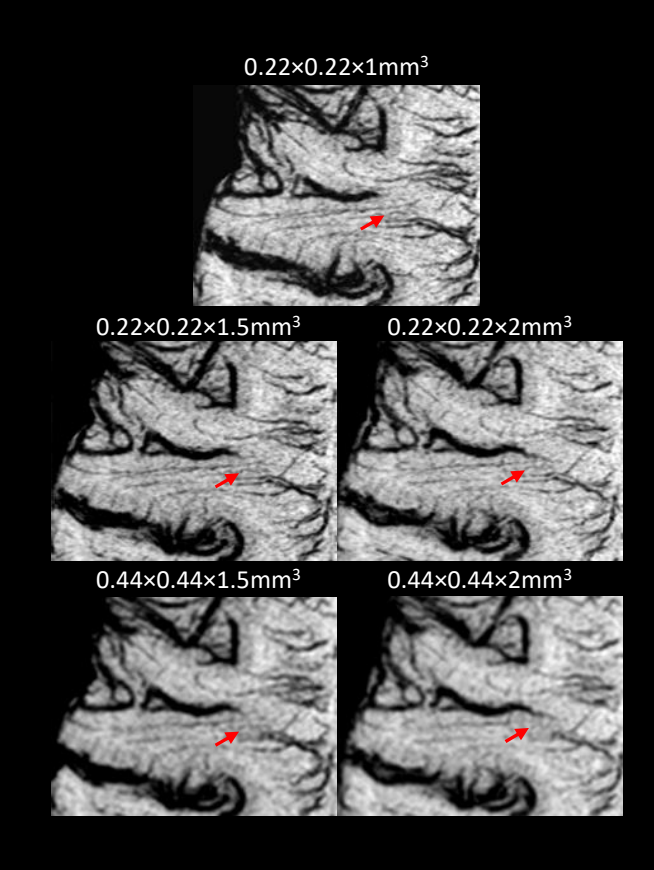
With USPIO, dose, TE, resolution, vessel size all become inter-related and understanding the final response requires careful modeling.

For TE=20ms and a 4mg/kg dose on 7T, we can see vessels as small as one-quarter the voxel size. <u>So, 200um resolution should allow us to see 50um vessels.</u>

MICRO Imaging: Imaging Resolution vs Vessel Visibility

USPIO dose = 4mg/kg of Ferumoxytol; $B_0 = 3T$

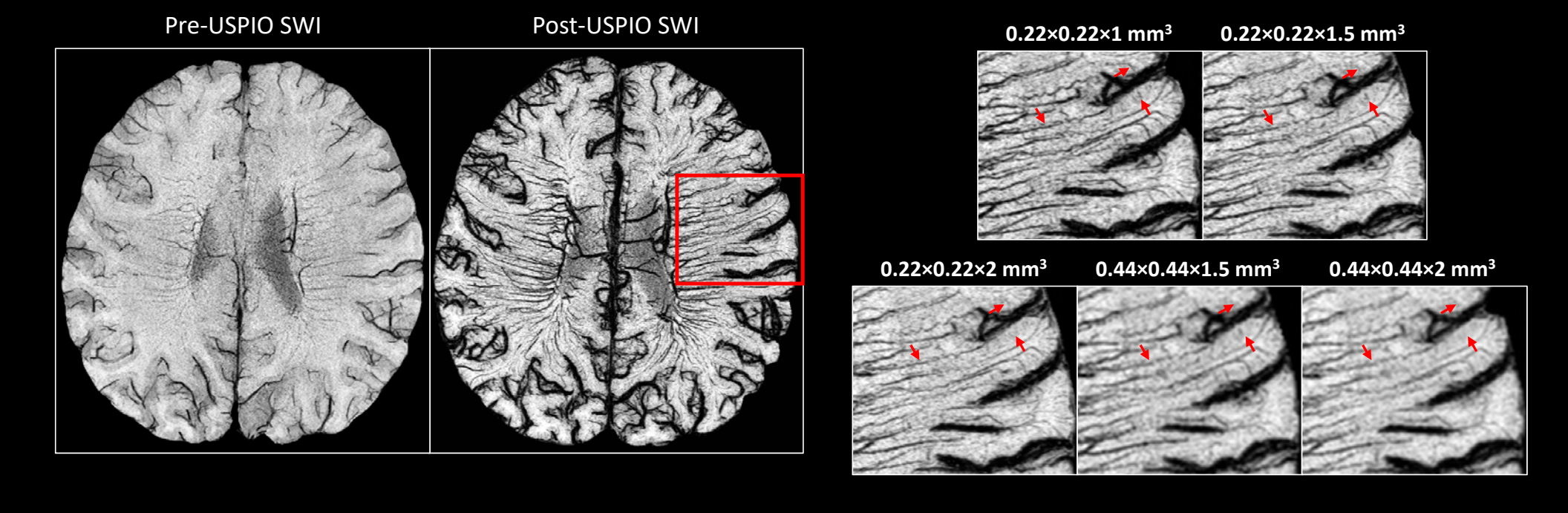




The higher the imaging resolution, the better the detectability of microvasculature

MICRO Imaging: Imaging Resolution vs Vessel Visibility

USPIO dose = 4mg/kg of Ferumoxytol; $B_0 = 3T$



The higher the imaging resolution, the better the detectability of microvasculature

Ferumoxytol enhanced MRAV on 7T

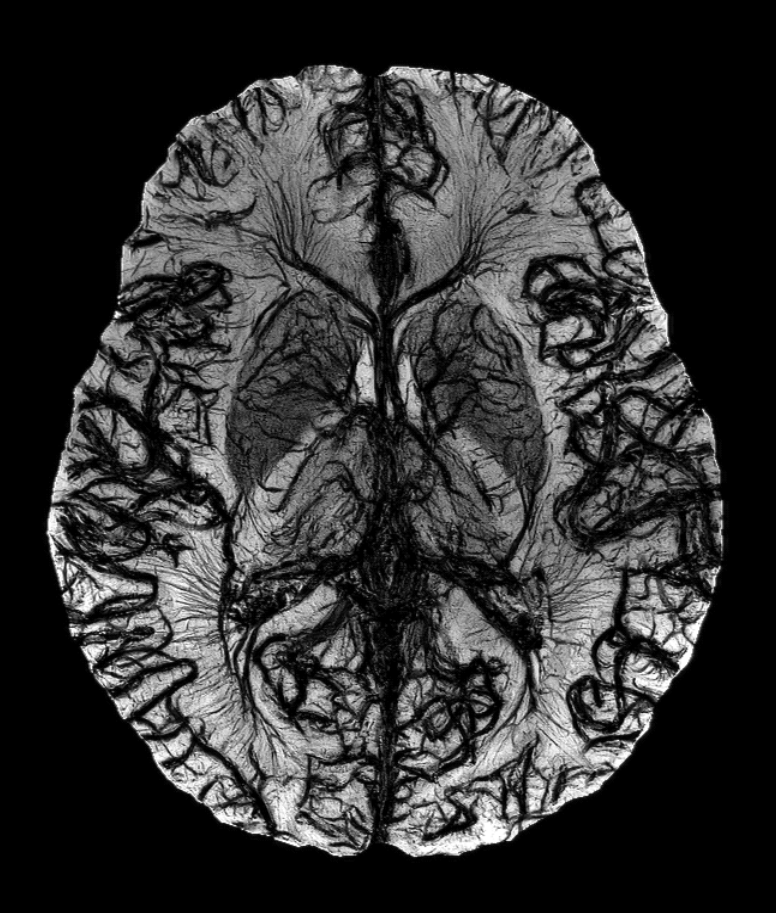


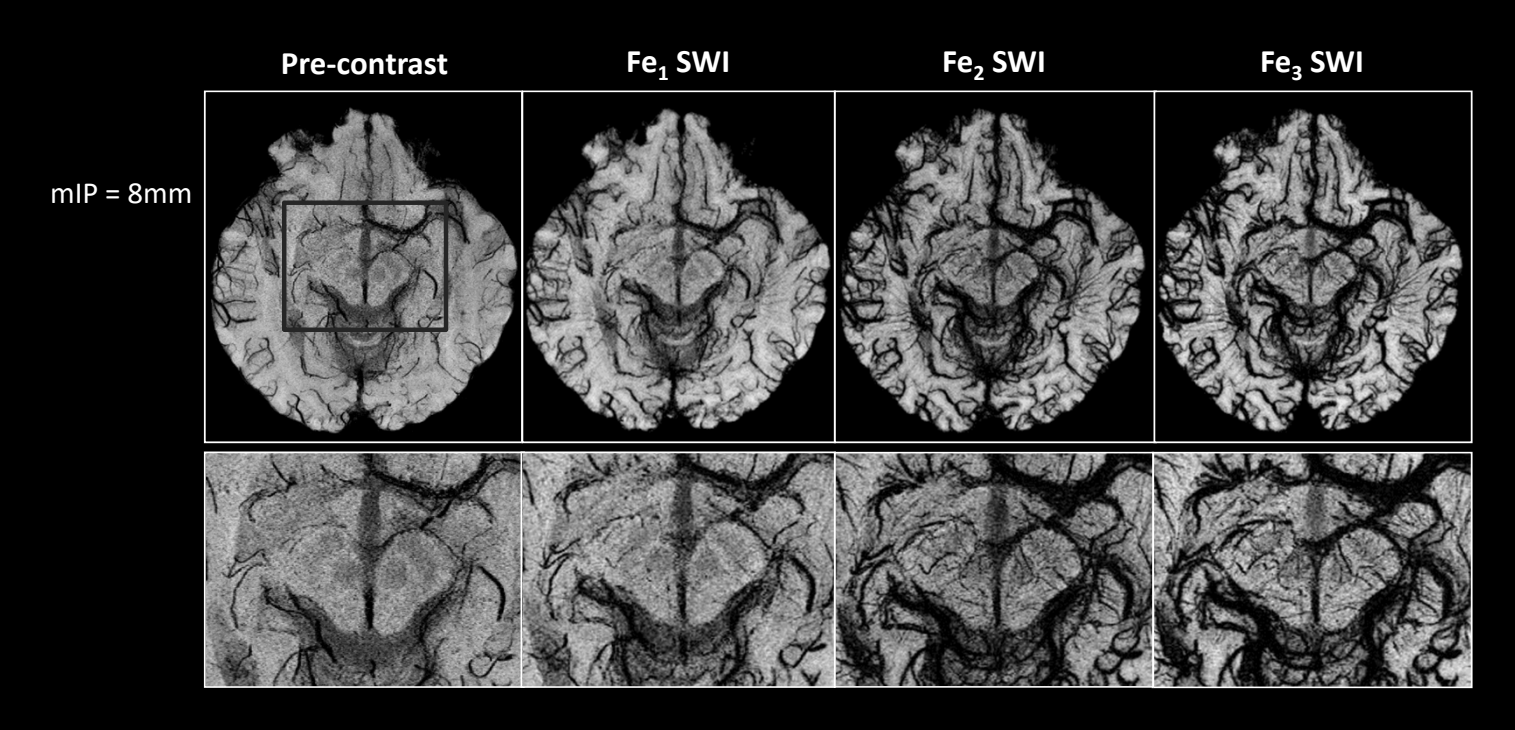
Image courtesy of Yulin Ge and NYU.

3T versus 7T MICRO Imaging

- Given the saturation effects of Ferumoxytol, one could in theory use MICRO at any of 1.5T, 3T and 7T field strengths
- But, high fields offer a linear increase in SNR
- We can double the in-plane resolution at 7T and still maintain the same SNR as at 3T
 - SNR α B $_o$
 - SNR $\alpha \sqrt{(N_x \times N_y)}$
- From a simple practical standpoint, we can already do very well at 3T as shown here, but we can in-principle do a better job at 7T

Applications of MICRO Imaging: Midbrain Microvasculature

MICRO Protocol for Acquiring USPIO-enhanced SWI on 3T

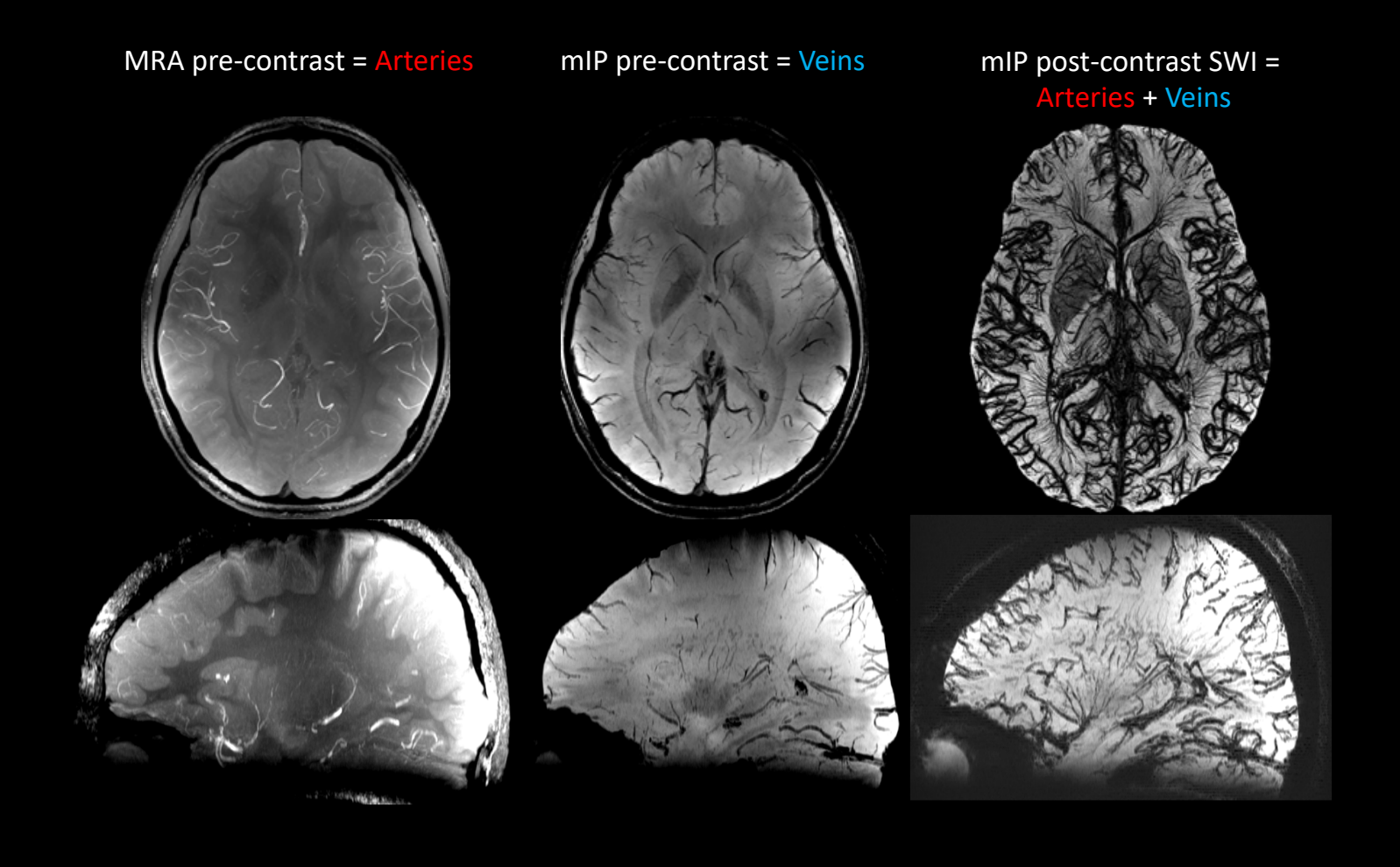


Imaging parameters:

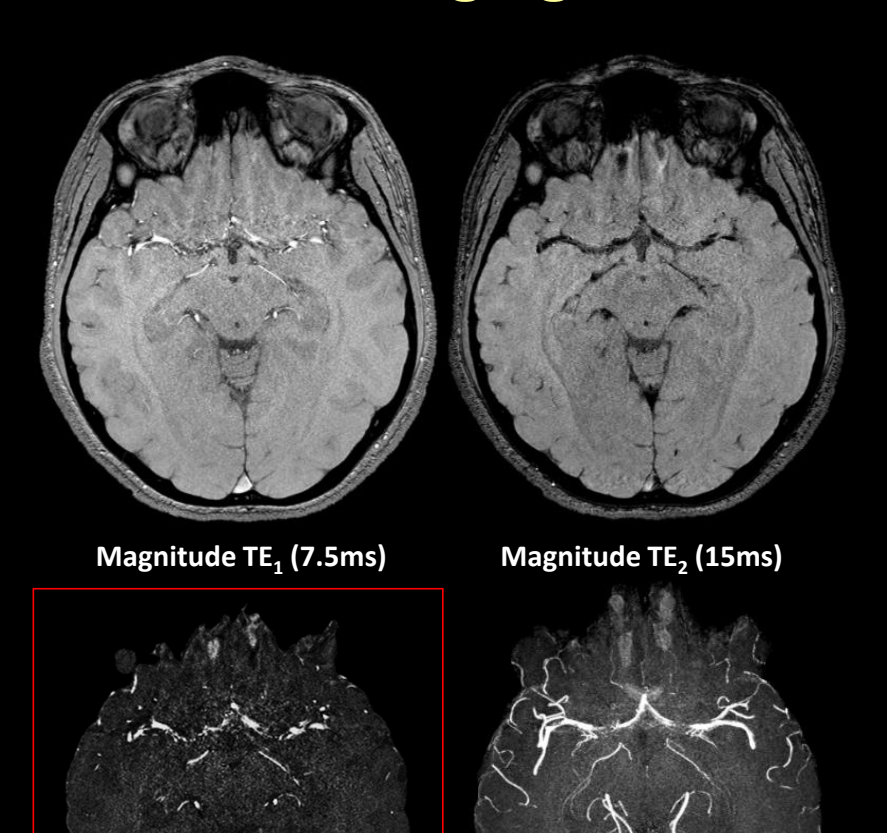
 $TE_1/TE_2/TR = 7.5/15/27ms$, Bandwidth = 180Hz/pxl, number of slices = 96, flip angle = 12°; voxel size = $0.22\times0.44\times1mm^3$ Acquisition time for each sequence = 11 mins, GRAPPA = 2/36 Final **Ferumoxytol** dose = 4mg/kg, <u>Dose delivery time = 21-23 mins</u>

Mapping the Macro-vasculature: MRA and MRV

Imaging the Arteries and Veins with MICRO



Imaging the Arteries with dual-echo GRE



MIP (8mm)

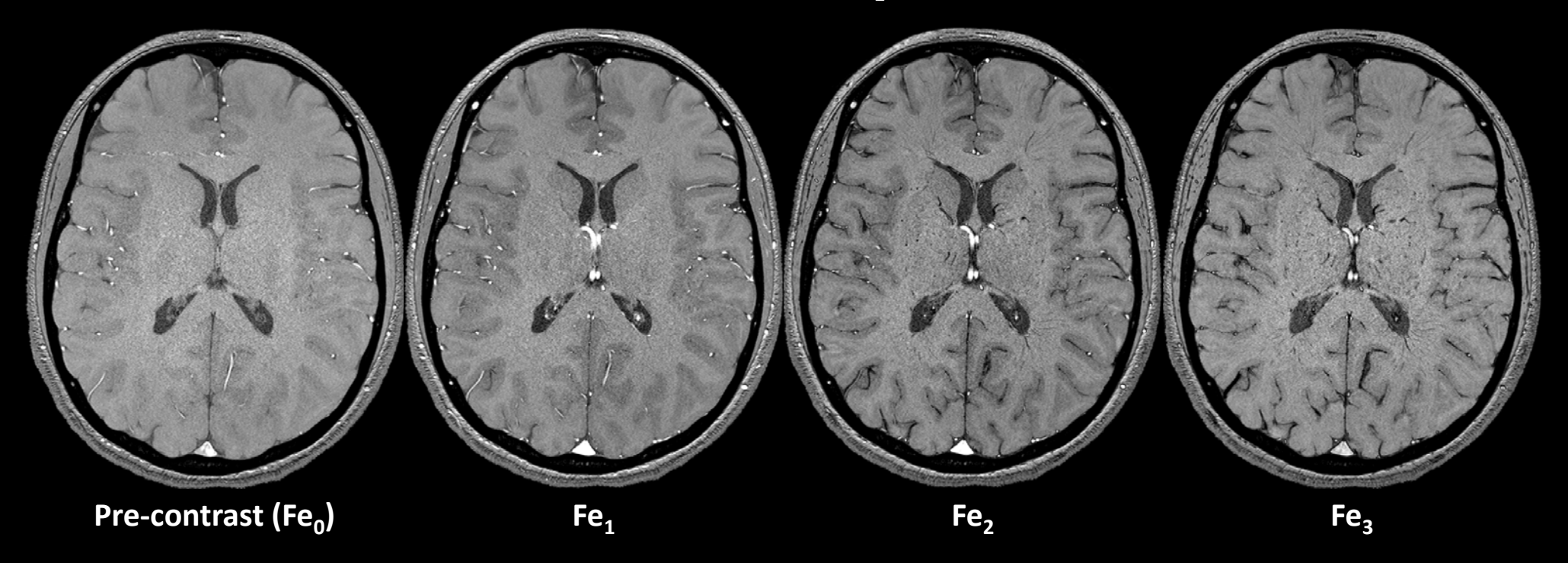
 $TE_1^2 - \alpha \cdot TE_2^2$

Improved MRA from a ME rephased TE₁ and dephased TE₂

Non-linearly subtracting TE₂ data from TE₁ data yields much more information on the presence of the small arteries

Magnitude Signal at Different Time Points

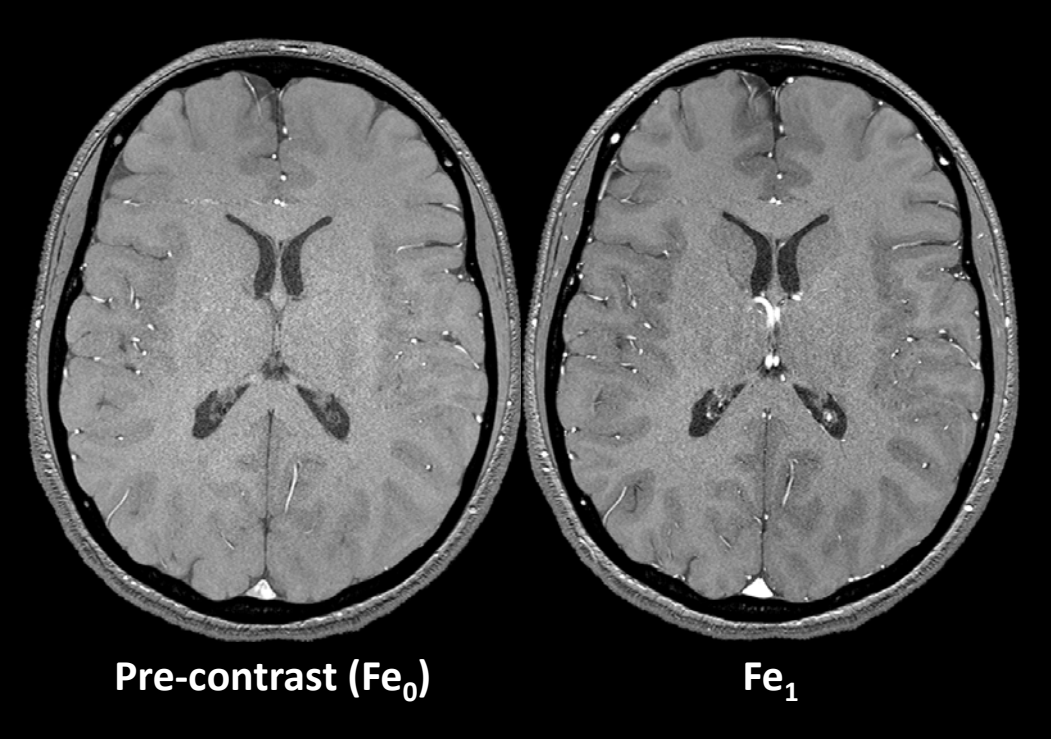
Magnitude TE₁

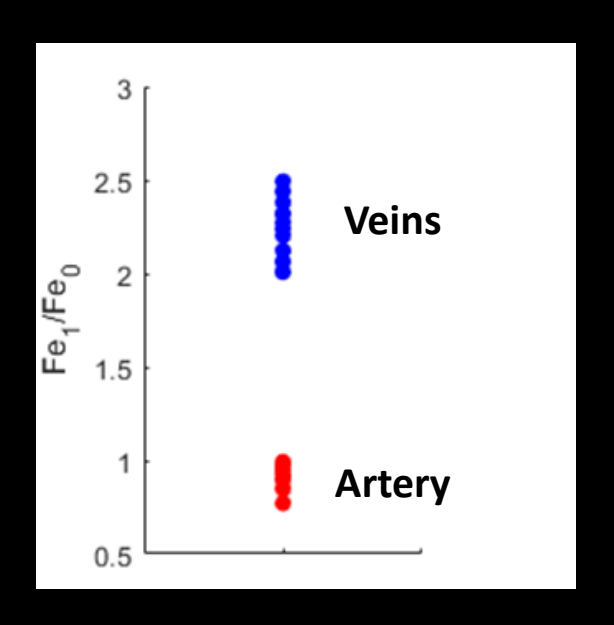




T₁-shortening due to Ferumoxytol: Venous Enhancement

Magnitude TE₁

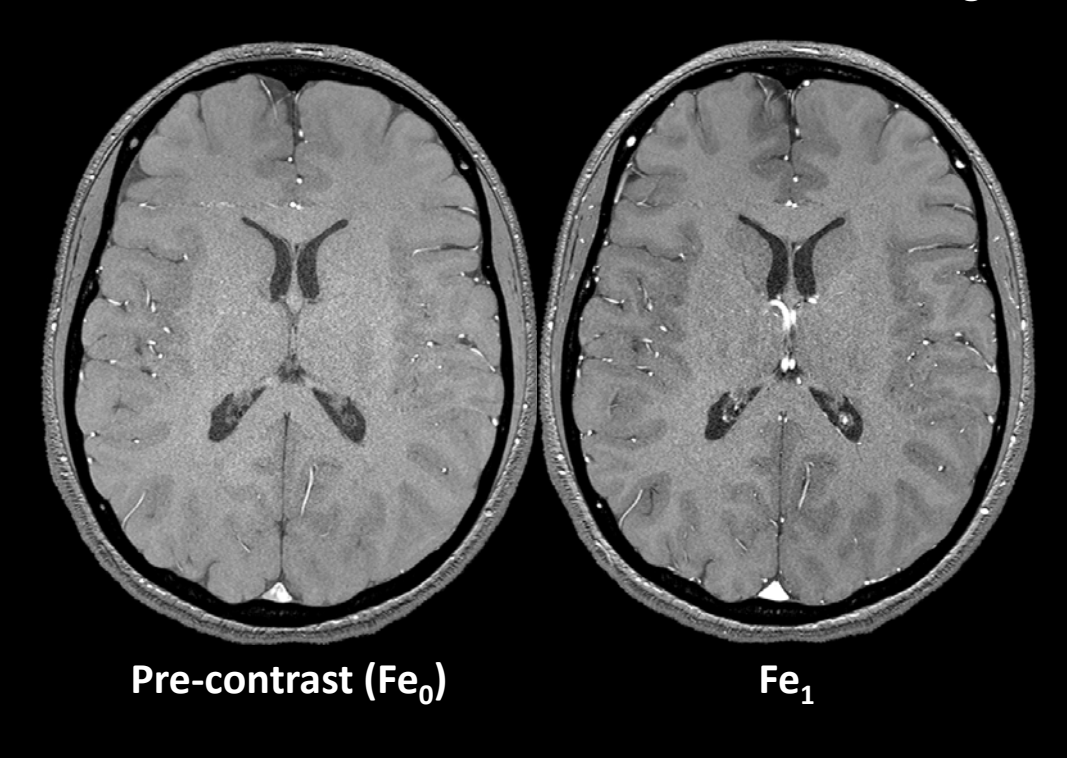


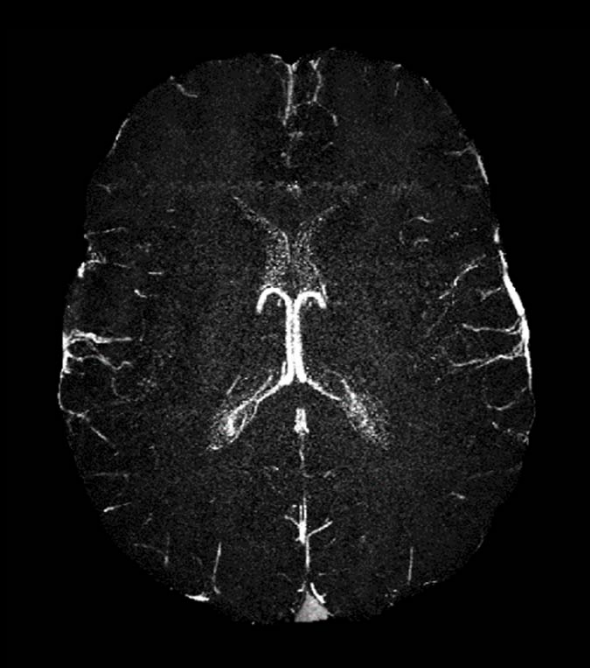




T₁-shortening due to Ferumoxytol: Venous Enhancement

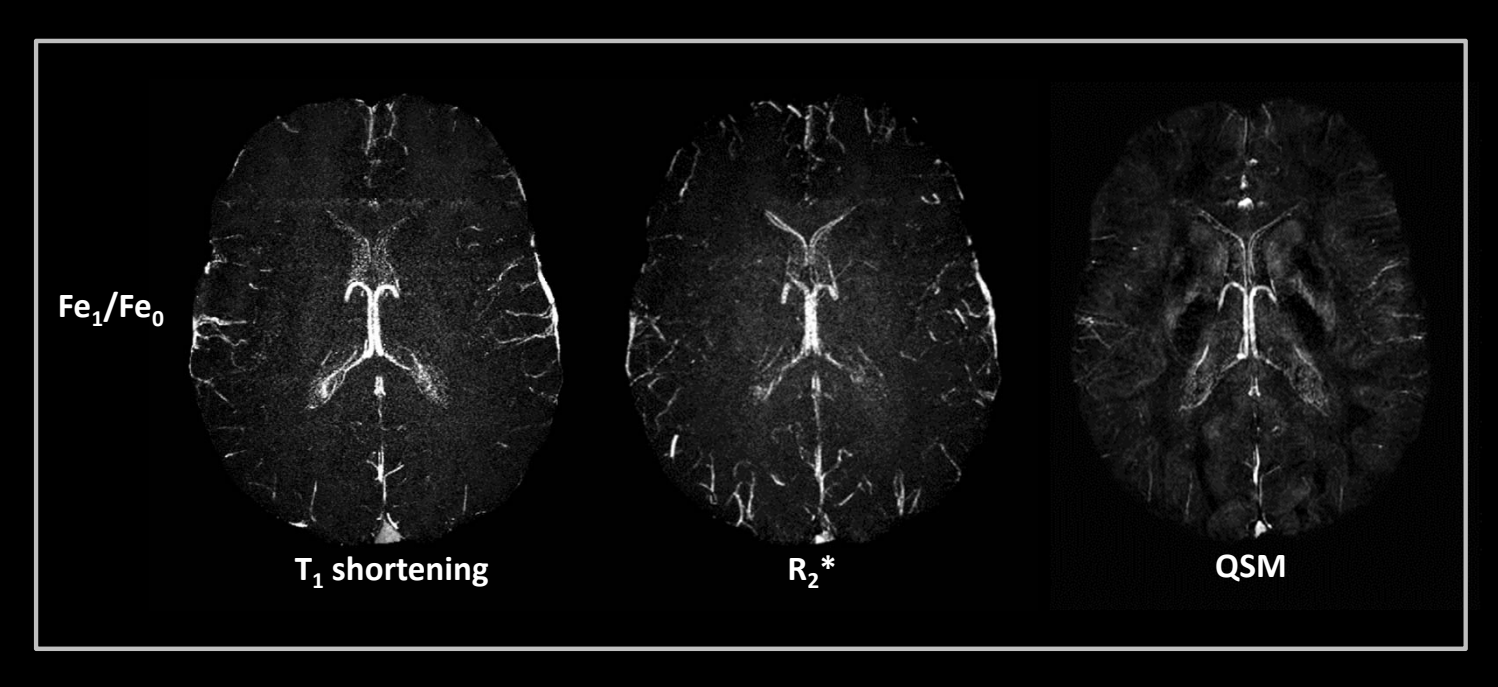
Magnitude TE₁

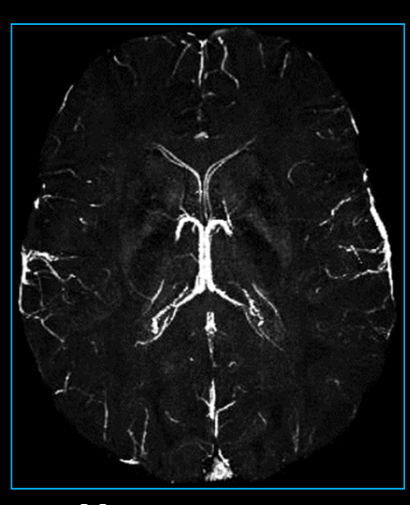






Imaging the Veins with MICRO

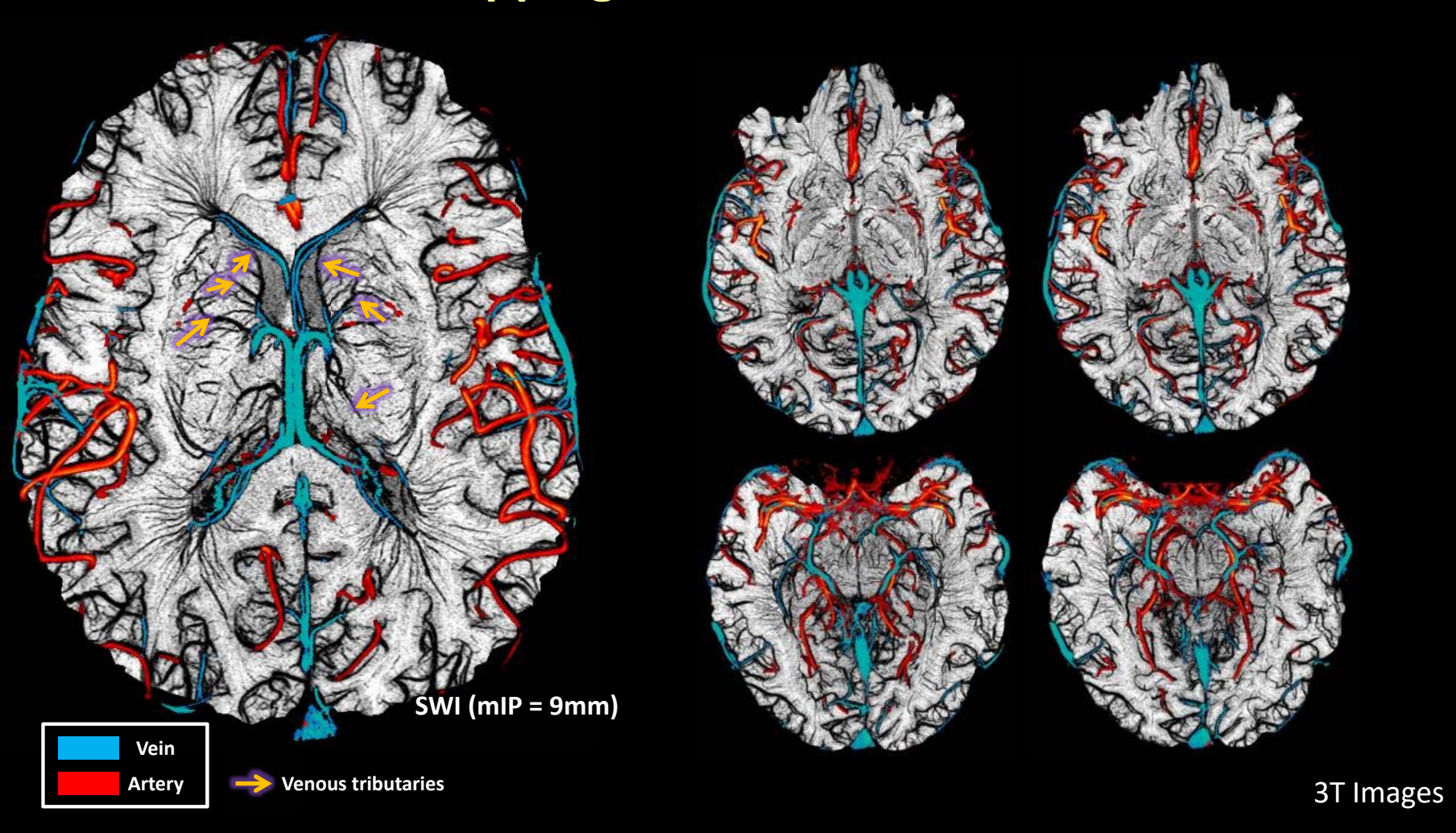




Mean venous map

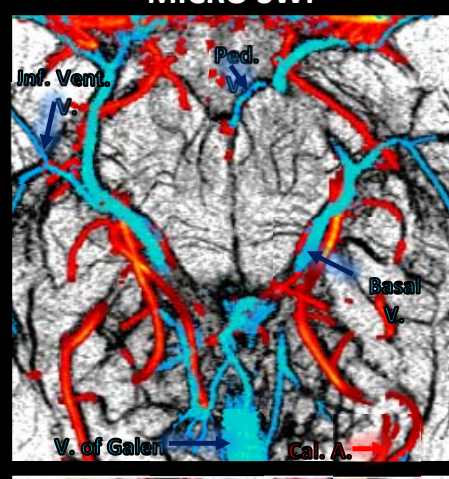
Using the first hand MRA and these final mean venous maps, we can begin to identify the major arteries and veins in MICRO.

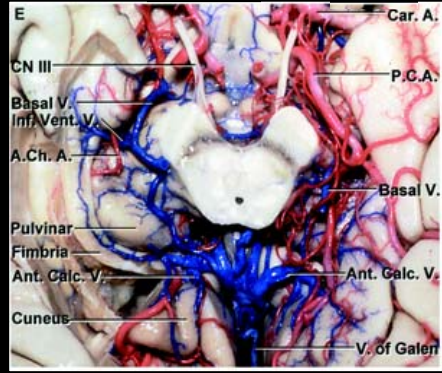
Mapping Cerebral Vessels



Comparison of MICRO and Cadaver brain data: Midbrain

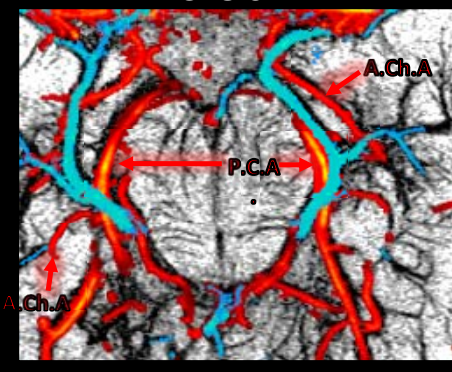
MICRO SWI

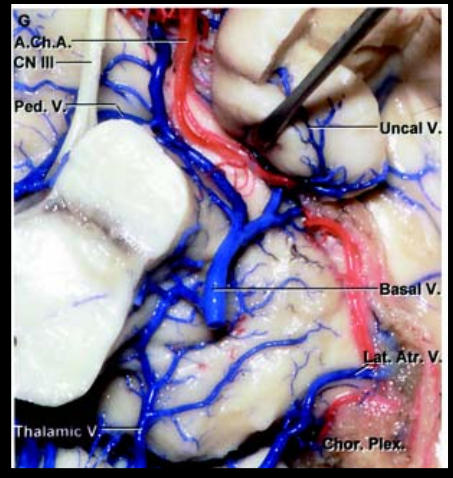




Cadaver data

MICRO SWI



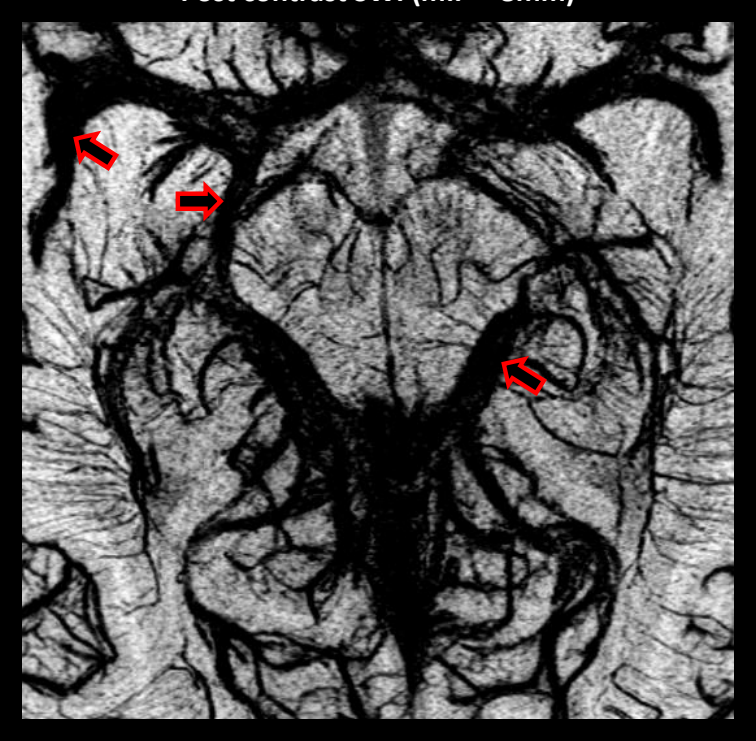


Cadaver data

Albert L. Rhoton, Jr., M.D., The Cerebral Veins, *Neurosurgery*, Volume 51, Issue suppl_4, 1 October 2002, Pages S1–159–S1–205

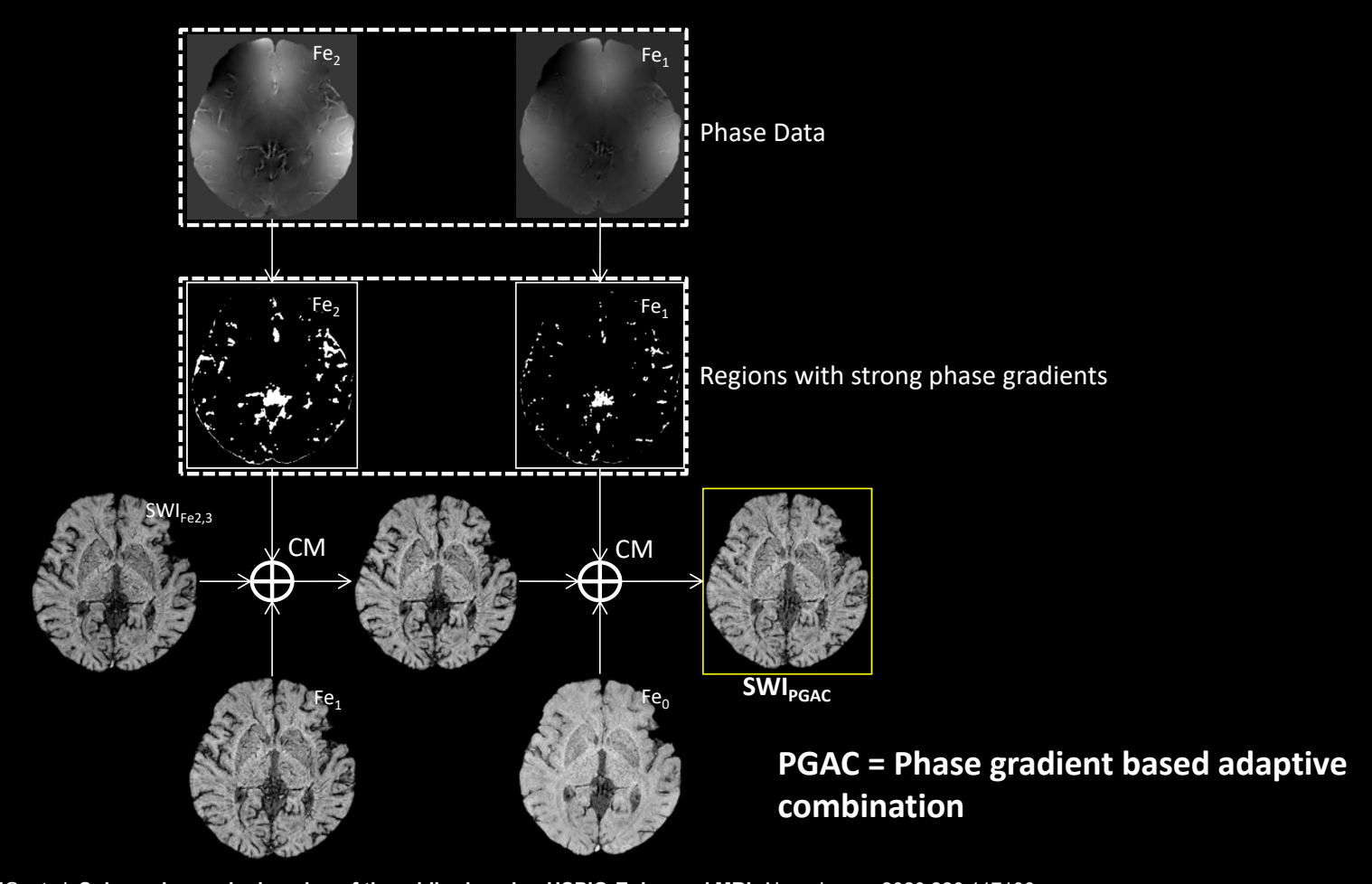
Dynamic Combination of USPIO-SWI data

Post contrast SWI (mIP = 8mm)



Buch S, Wang Y, Park MG, et al. Subvoxel vascular imaging of the midbrain using USPIO-Enhanced MRI. Neuroimage. 2020;220:117106.

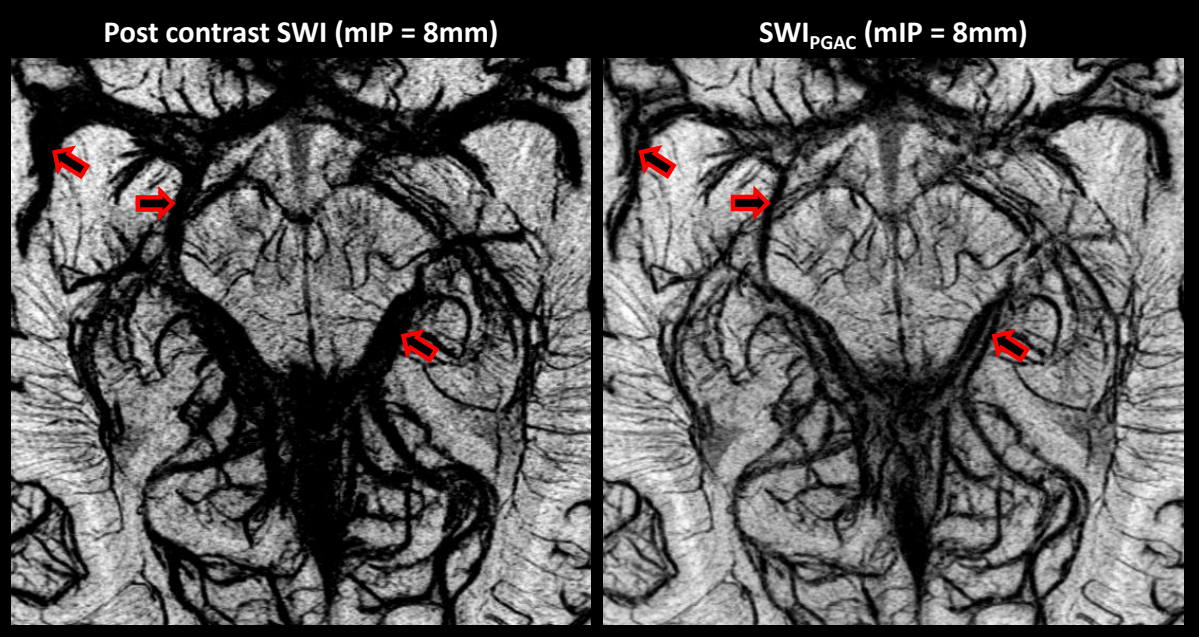
Dynamic Combination of USPIO-SWI data



Buch S, Wang Y, Park MG, et al. Subvoxel vascular imaging of the midbrain using USPIO-Enhanced MRI. Neuroimage. 2020;220:117106.

Dynamic Combination of USPIO-SWI data

To reduce the blooming artifact and better identify vessels



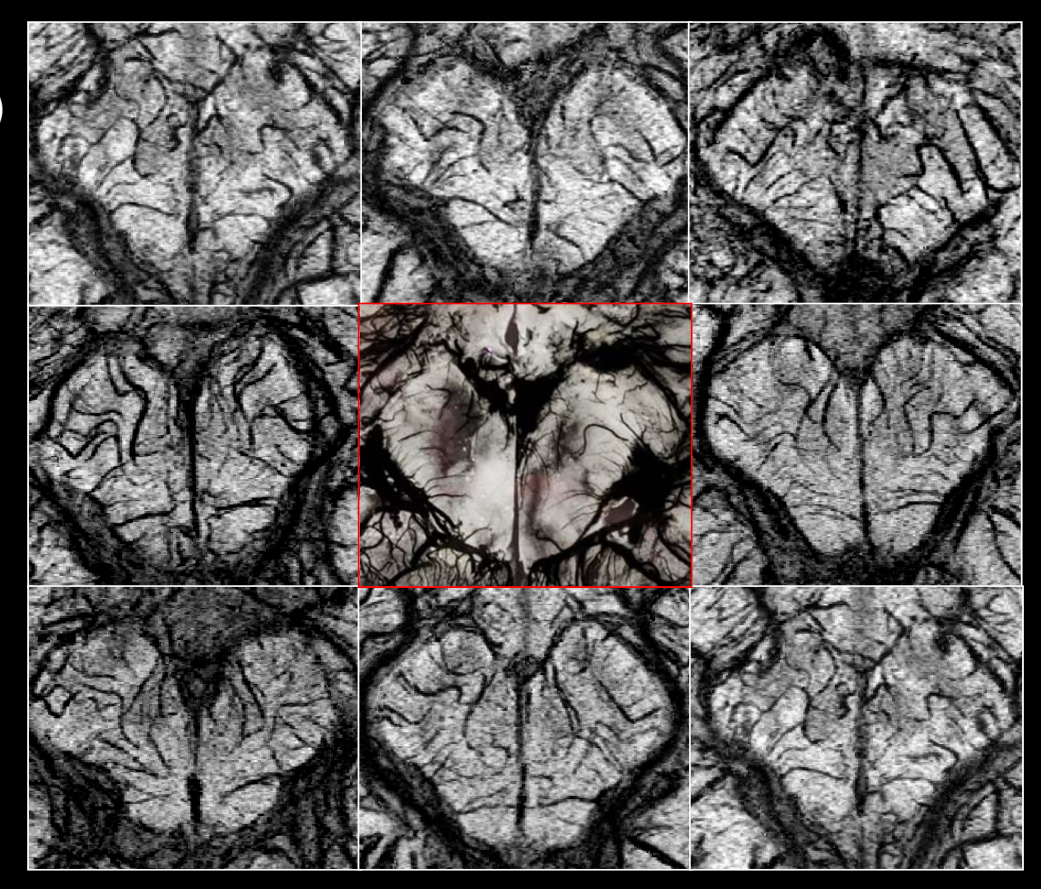
PGAC = Phase-gradient based adaptive combination

3T Images

Buch S, Wang Y, Park MG, et al. Subvoxel vascular imaging of the midbrain using USPIO-Enhanced MRI. Neuroimage. 2020;220:117106.

Comparison of MICRO and Cadaver brain dye injection

3T SWI (mIP=8mm)

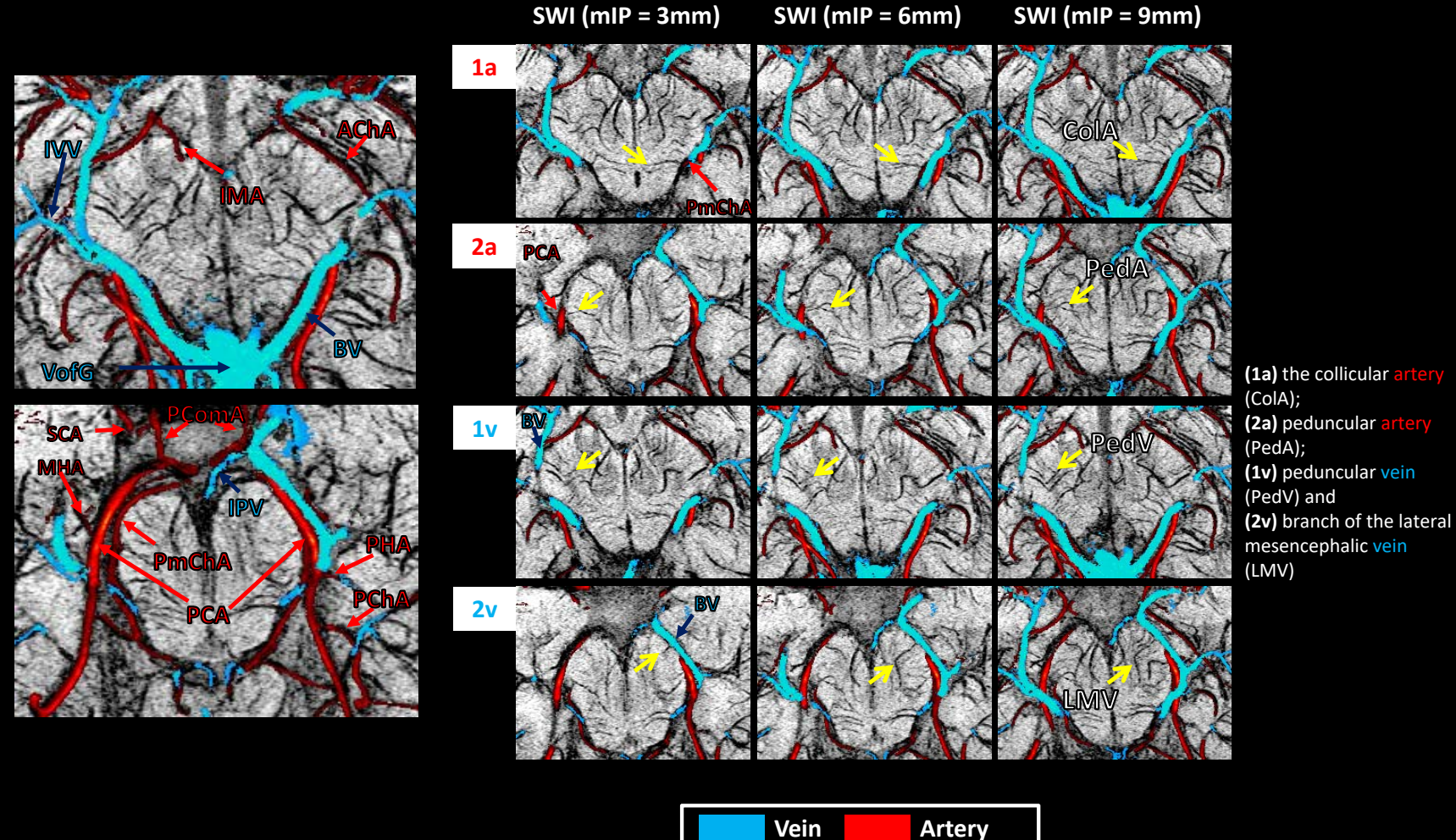


Center image: In vitro angiogram

Georges Salamon; J M Corbaz Atlas de la vascularisation arterielle du cerveau chez l'homme

Buch S, et al. **Subvoxel vascular imaging of the midbrain using USPIO-Enhanced MRI.** *Neuroimage*. 2020;220:117106.

Mapping the Connectivity of the Midbrain Vessels



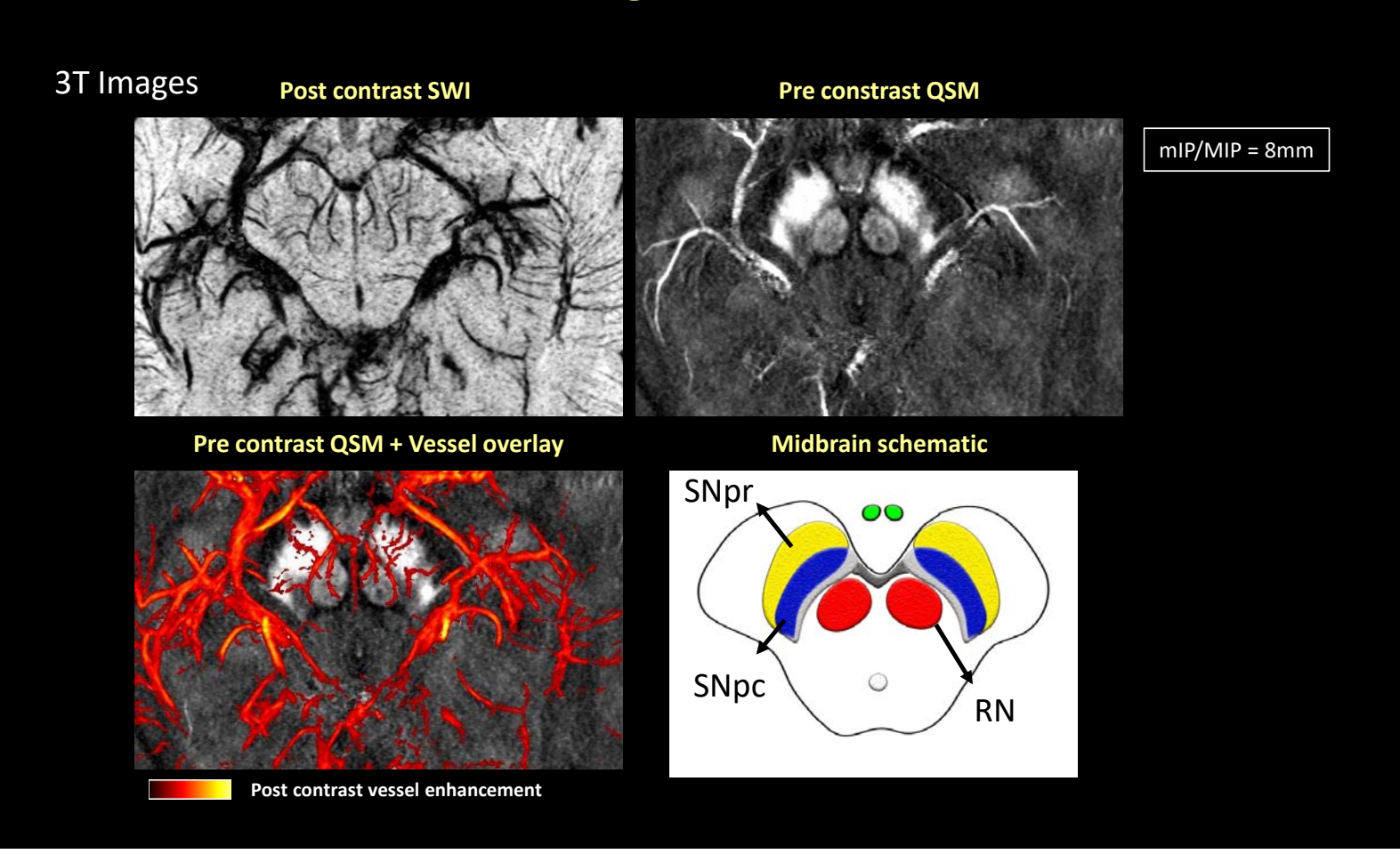
Major brainstem arteries:

AChA = anterior choriodal artery, IMA = inferior medial mesencephalic, MHA = medial hippocampal, PCA = posterior cerebral, PChA = posterior choroidal, PComA = posterior communicating, PHA = posterior hippocampal, PmChA = posterior-medial choriodal, SCA = superior cerebral artery.

Major brainstem veins:

BV = basal vein, IVV = inferior ventricular vein, IPV = interpeduncular vein, VofG = vein of Galen.

Mapping the *Midbrain-Hippocampal* Vasculature using MICRO

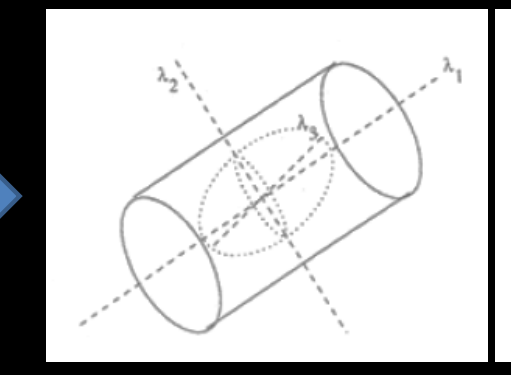


Mapping the Micro-vasculature

Utilizing The Frangi Vesselness Filter to Suppress Background Signal

Hessian Matrix

$$H(f) = \begin{bmatrix} \frac{\partial^2 f}{\partial x_1^2} & \frac{\partial^2 f}{\partial x_1 \partial x_2} & \cdots & \frac{\partial^2 f}{\partial x_1 \partial x_n} \\ \frac{\partial^2 f}{\partial x_2 \partial x_1} & \frac{\partial^2 f}{\partial x_2^2} & \cdots & \frac{\partial^2 f}{\partial x_2 \partial x_n} \\ \vdots & \vdots & \ddots & \vdots \\ \frac{\partial^2 f}{\partial x_n \partial x_1} & \frac{\partial^2 f}{\partial x_n \partial x_2} & \cdots & \frac{\partial^2 f}{\partial x_n^2} \end{bmatrix}$$



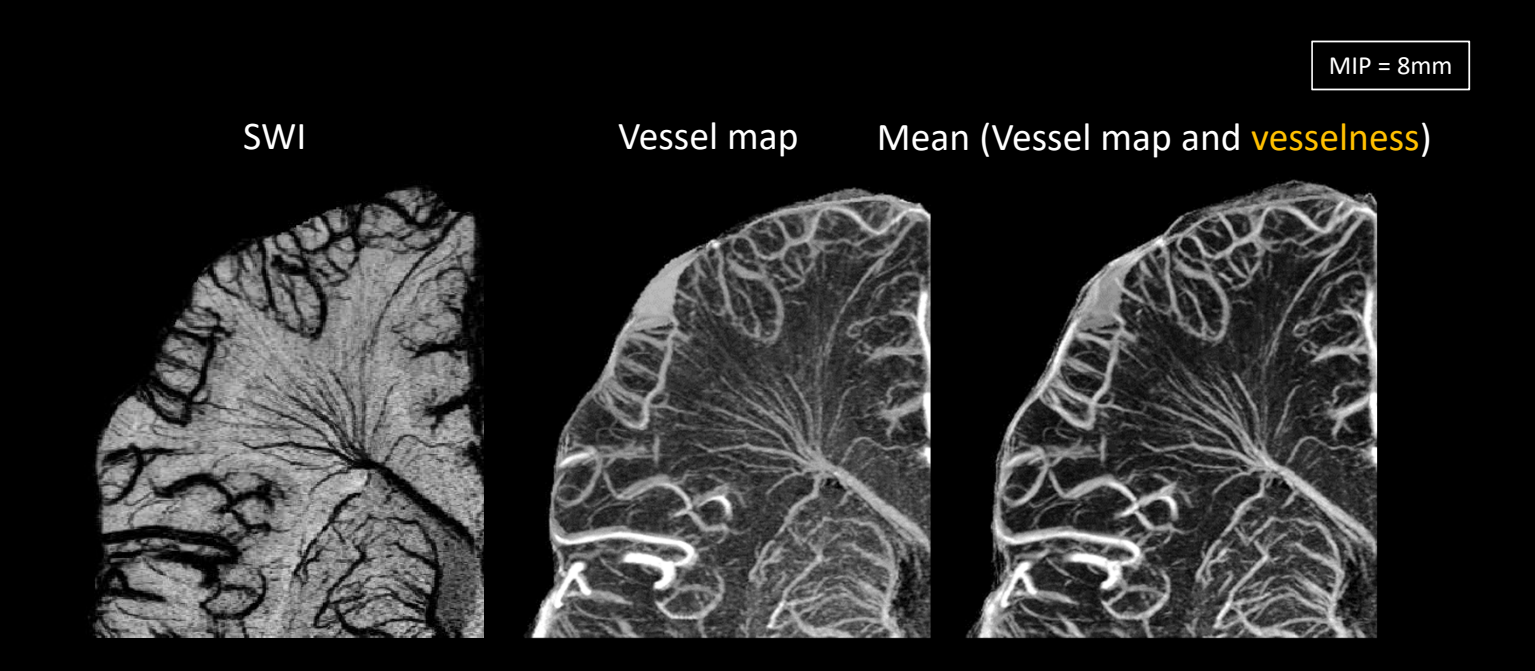
black	orientation pattern		3 <i>D</i>			2D	
٦		λ_3	λ_2	λ_1	λ_2	λ_1	
n	noisy, no preferred direction	N	N	N	N	N	
)	plate-like structure (bright)	Н-	L	L			
٦	plate-like structure (dark)	Н+	L	L			
	tubular structure (bright)	H-	H-	L	H-	L	
	tubular structure (dark)	H+	H+	L	H+	L	
)	blob-like structure (bright)	H-	H-	H-	Н-	H-	
	blob-like structure (dark)	H+	H+	H+	H+	H+	

$$R_{
m B}=rac{|\lambda_1|}{\sqrt{|\lambda_2\lambda_3|}} \quad R_{
m A}=rac{|\lambda_2|}{|\lambda_3|} \quad S=\sqrt{\lambda_1^2+\lambda_2^2+\lambda_3^2}.$$

$$V(\sigma) = \begin{cases} 0 & \text{if } \lambda_2 < 0 \text{ or } \lambda_3 < 0, \\ \left(1 - \exp\left(-\frac{R_A^2}{2\alpha^2}\right)\right) \exp\left(-\frac{R_B^2}{2\beta^2}\right) \left(1 - \exp\left(-\frac{S^2}{2c^2}\right)\right). \end{cases}$$

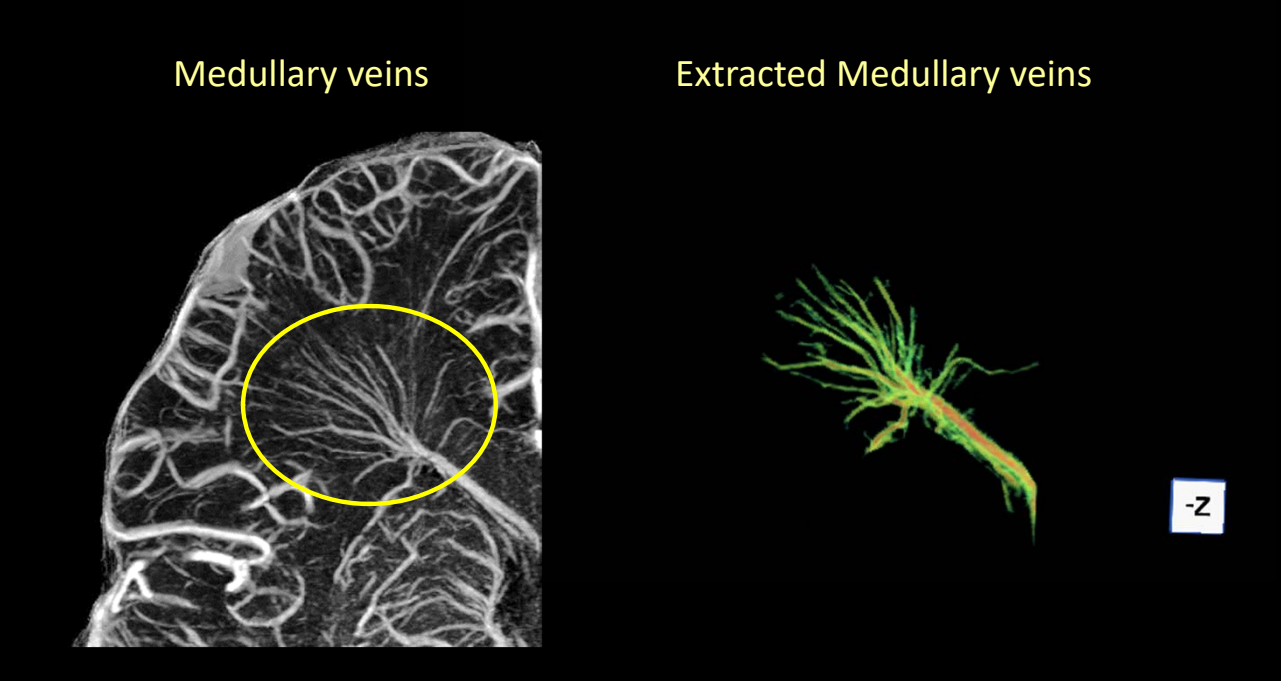
Frangi A.F., Niessen W.J., Vincken K.L., Viergever M.A. (1998) Multiscale vessel enhancement filtering. In: Wells W.M., Colchester A., Delp S. (eds) Medical Image Computing and Computer-Assisted Intervention — MICCAl'98. Lecture Notes in Computer Science, vol 1496. Springer, Berlin, Heidelberg

Utilizing The Frangi Vesselness Filter to Suppress Background Signal

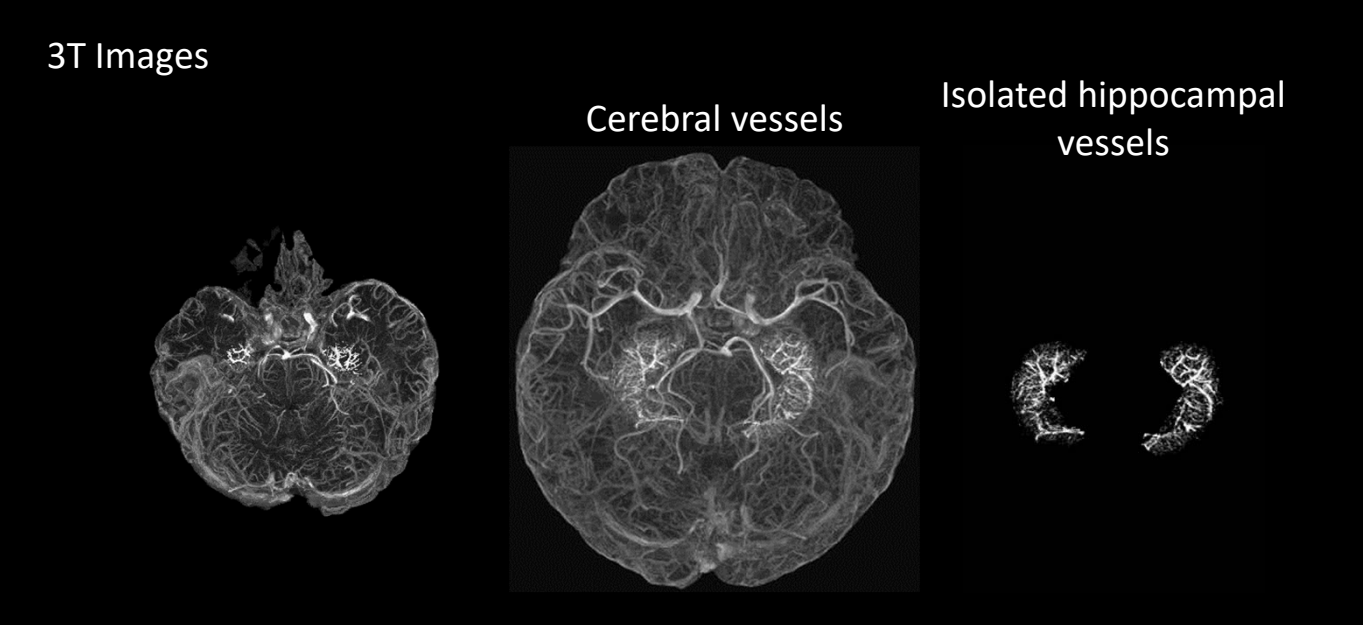


3T Images

Extracting the Cerebral Vasculature



Applications of MICRO Imaging: Hippocampal Microvasculature

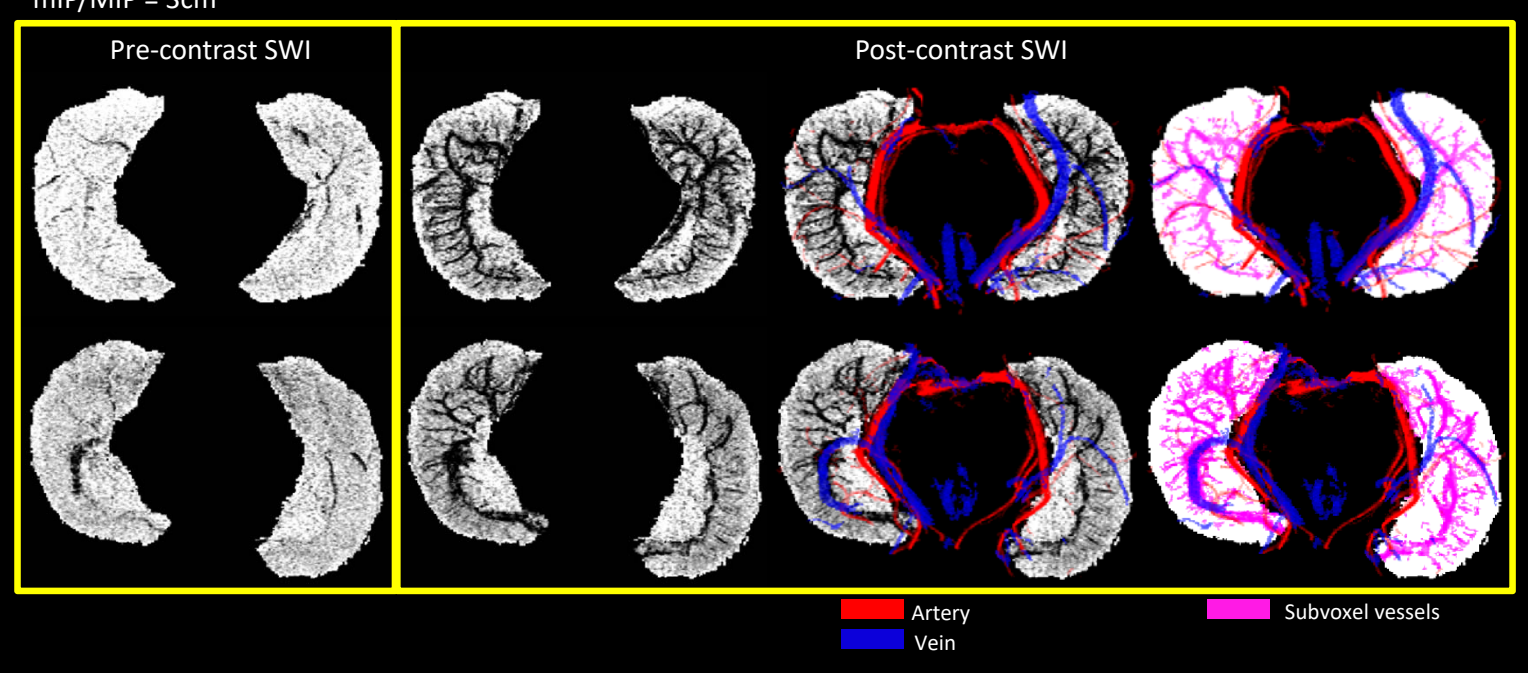


For the first time, we can isolate and visualize the vessels of the hippocampus *in vivo*

Hippocampus Vessel Extraction

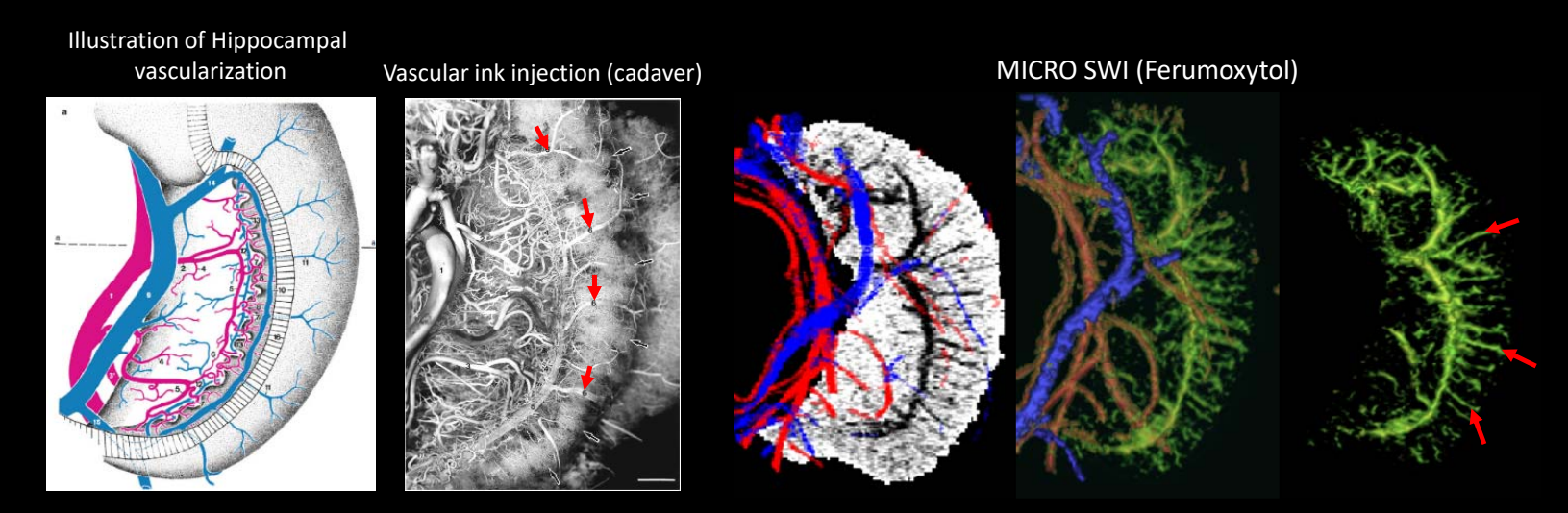
3T Images

mIP/MIP = 3cm



Hippocampal Macro- and Micro-vasculature

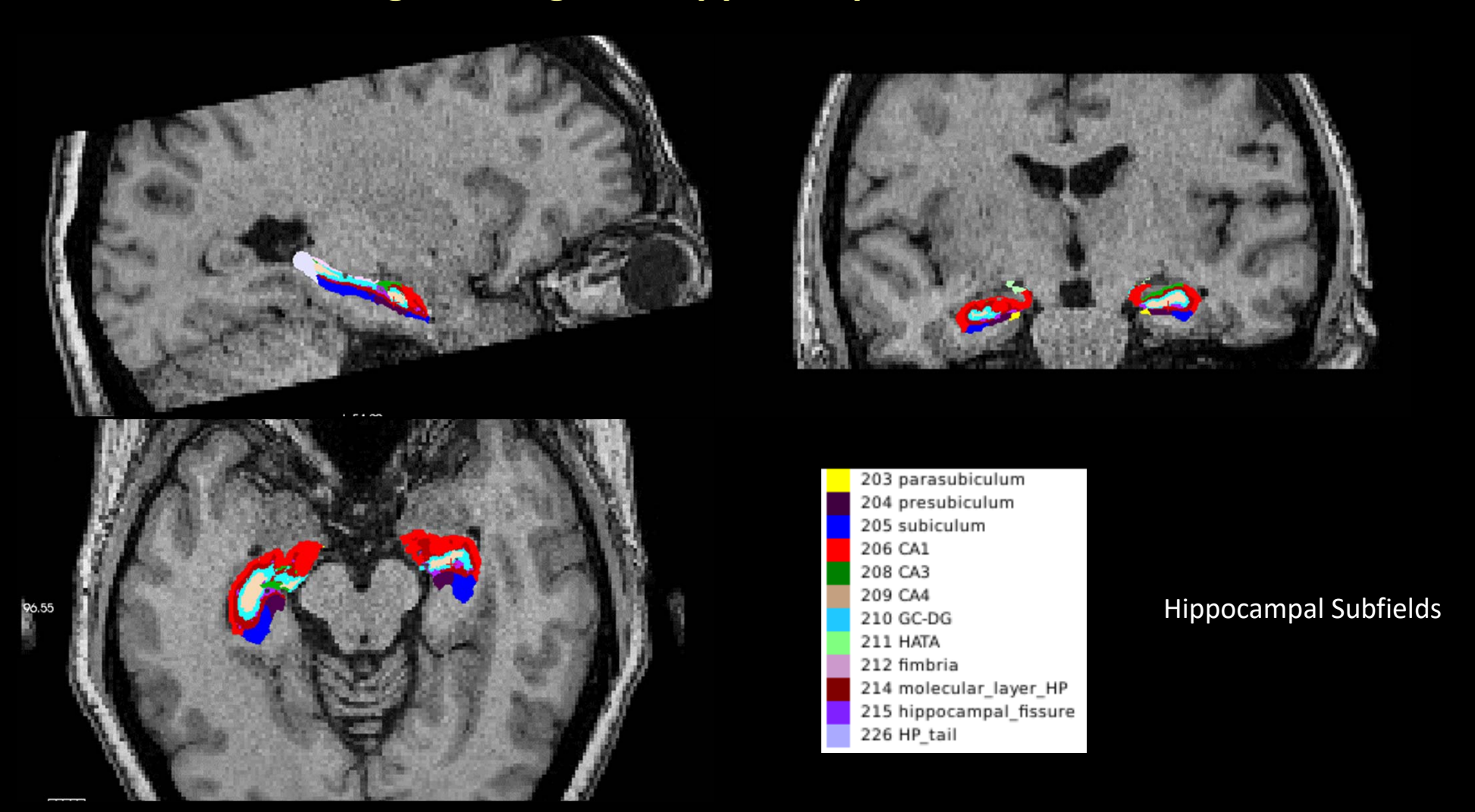
3T Images



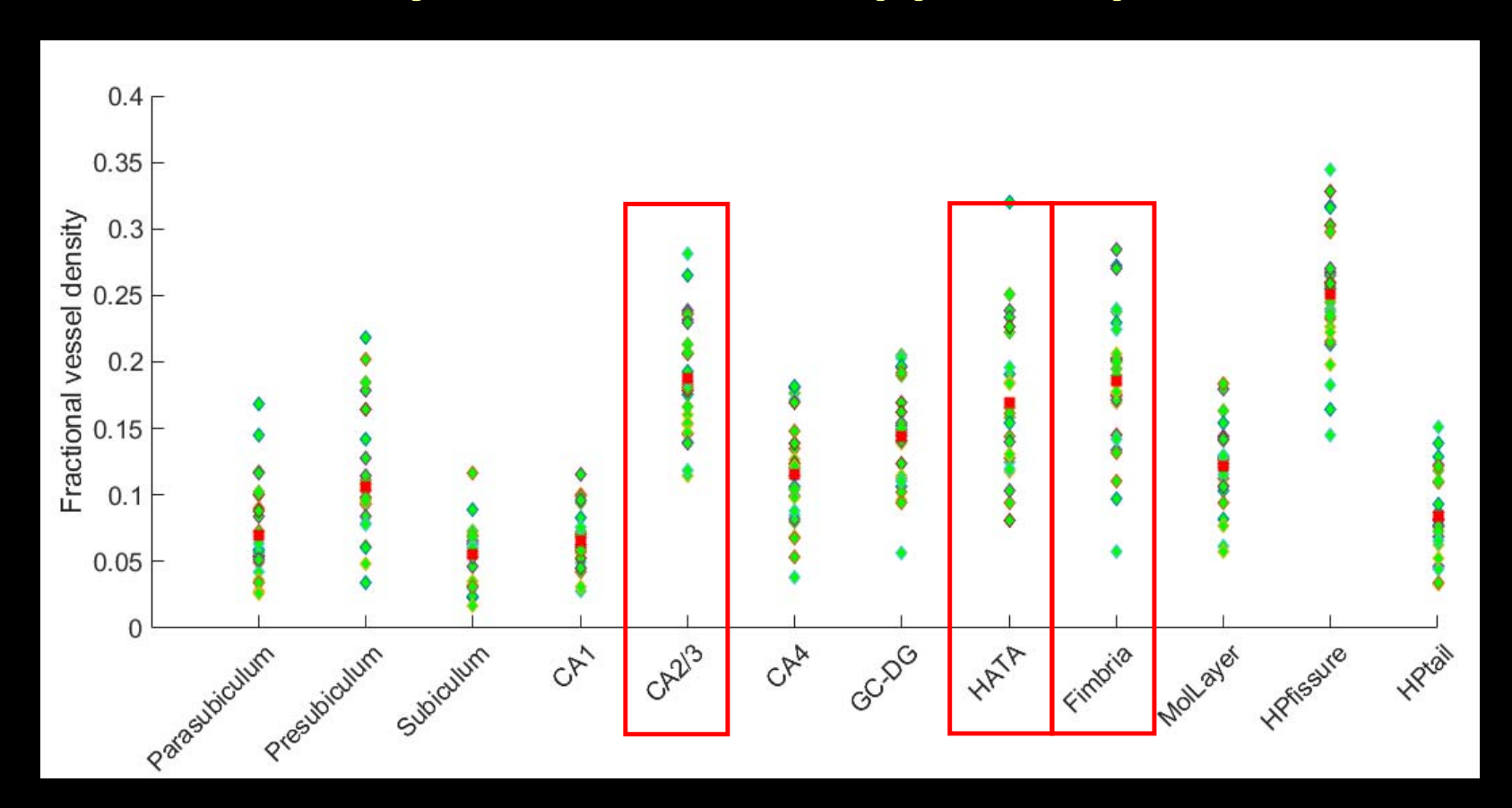
Duvernoy et al., The Human Hippocampus: Functional Anatomy, Vascularization and Serial Sections with MRI. 2013, 4th edition, Springer-Verlag Berlin Heidelberg, pg. 74 and 99.

→ Subependymal intra-hippocampal veins

Segmenting the Hippocampal Subfields

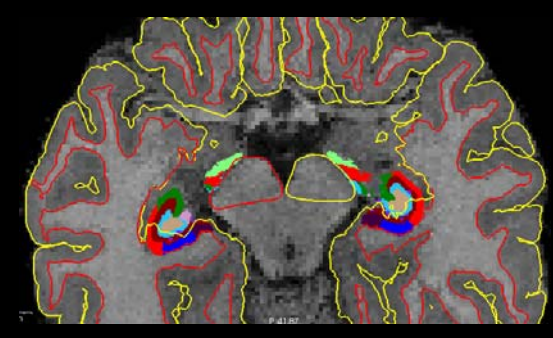


Vessel Density of Different Hippocampal Sub-fields

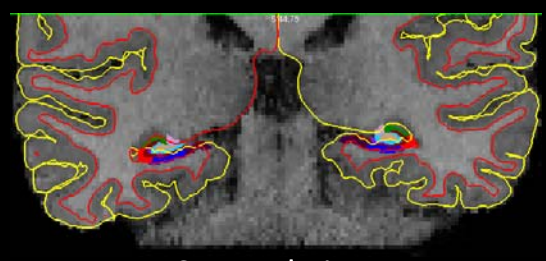


GC-DG = Granule cell layer of the dentate gyrus, HATA = Hippocampal-amygdaloid transition region, MolLayer = Molecular layer of HP

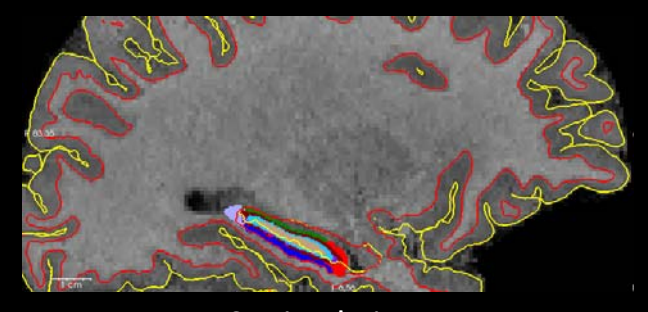
Hippocampal Subfields with Cortical Surface





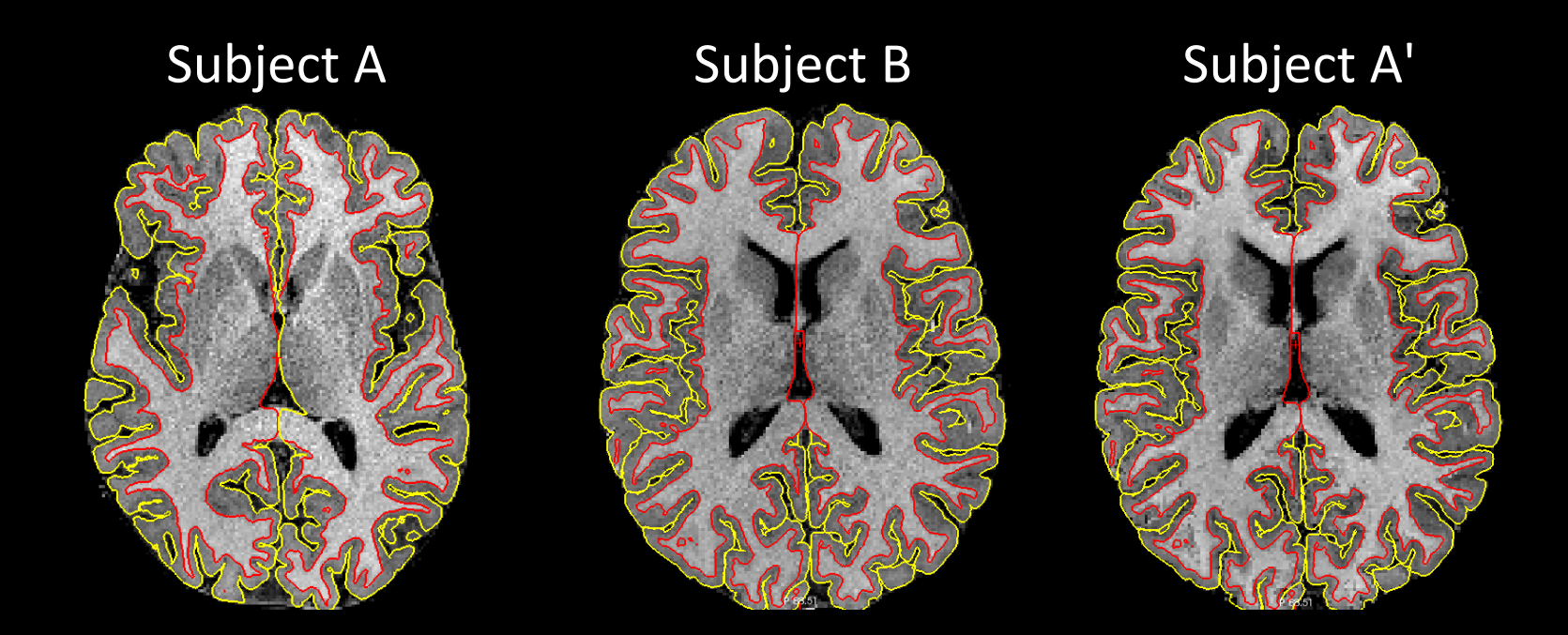


Coronal view



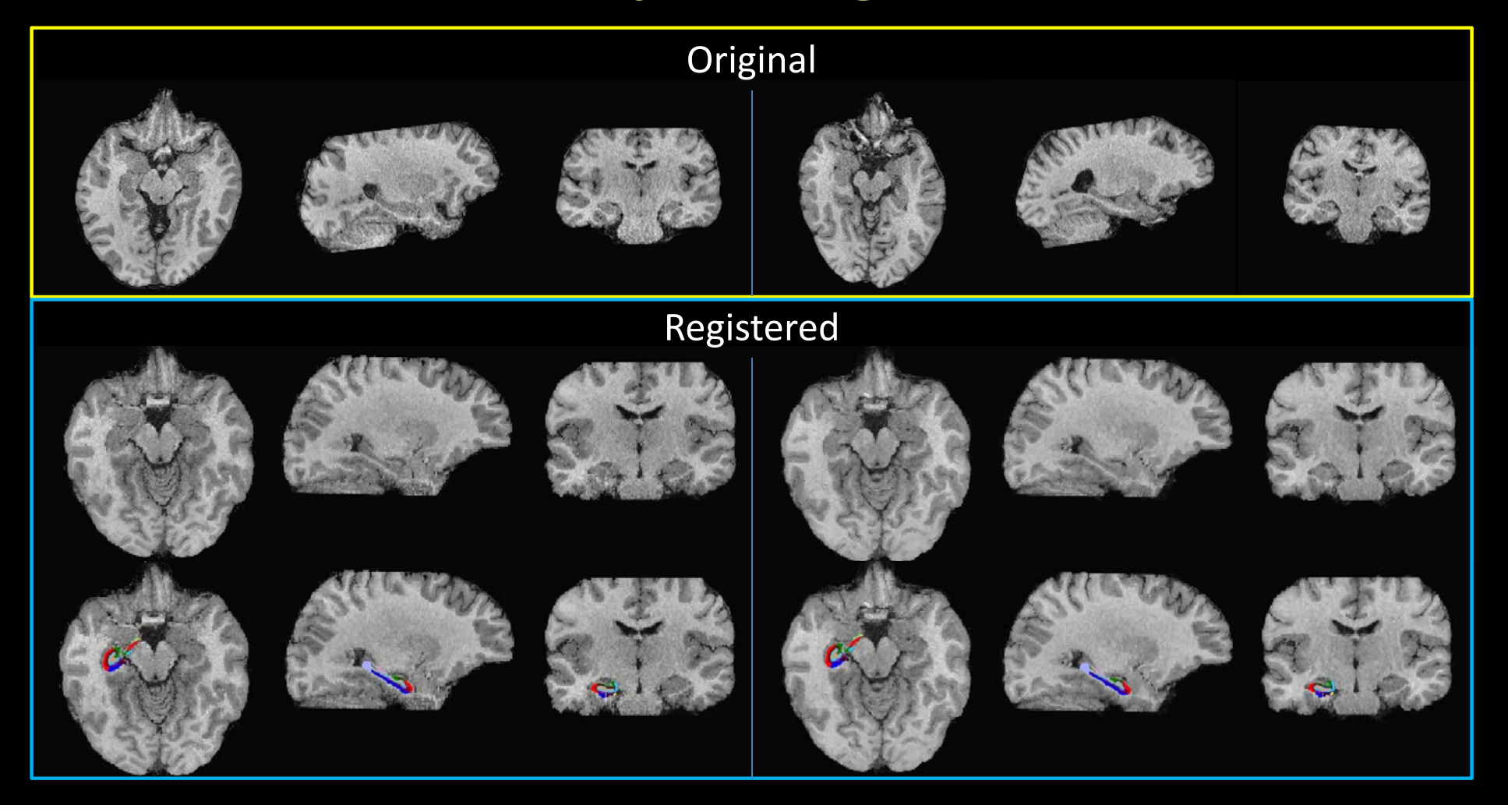
Sagittal view

Inter-subject Registration

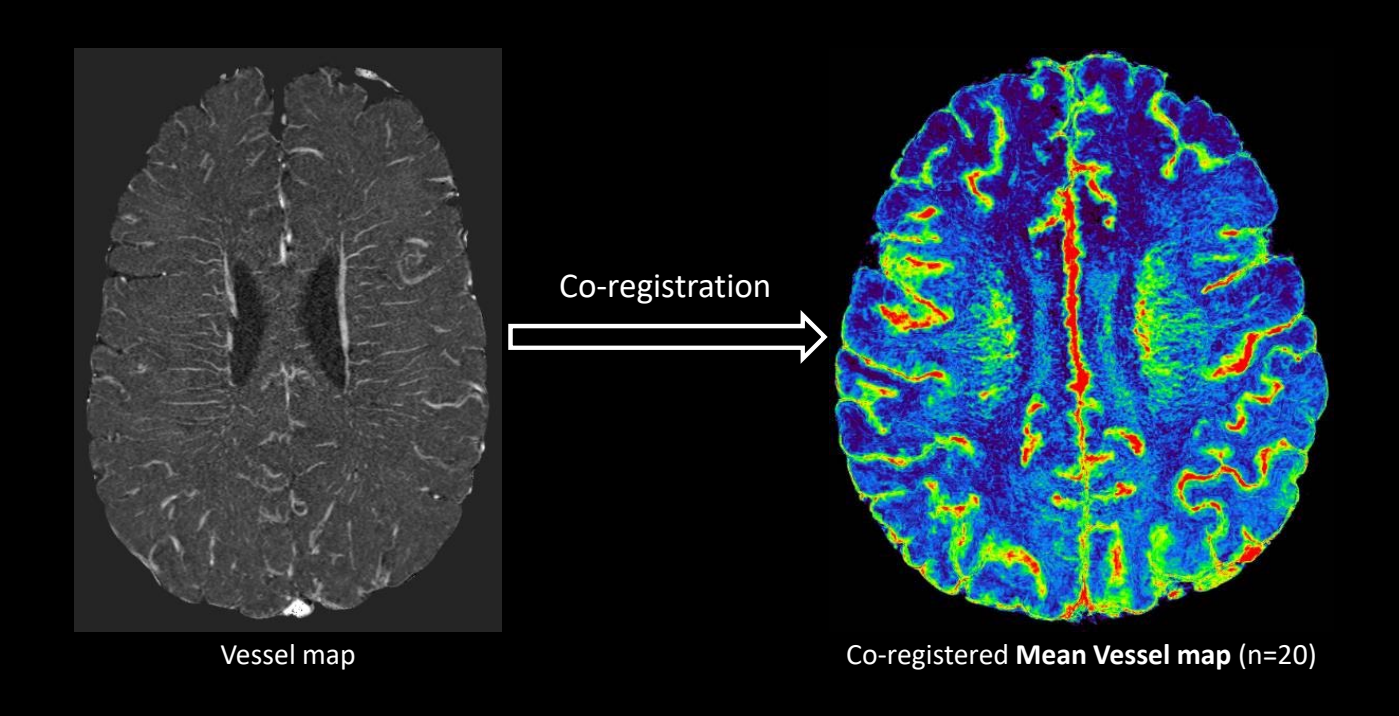


CVS registration: G.M. Postelnicu*, L. Zöllei*, B. Fischl: "Combined Volumetric and Surface Registration", IEEE Transactions on Medical Imaging (TMI), Vol 28 (4), April 2009, p. 508-522. L. Zöllei, A. Stevens, K. Huber, S. Kakunoori, B. Fischl: "Improved Tractography Alignment Using Combined Volumetric and Surface Registration", NeuroImage 51 (2010), 206-213

Inter-subject Registration

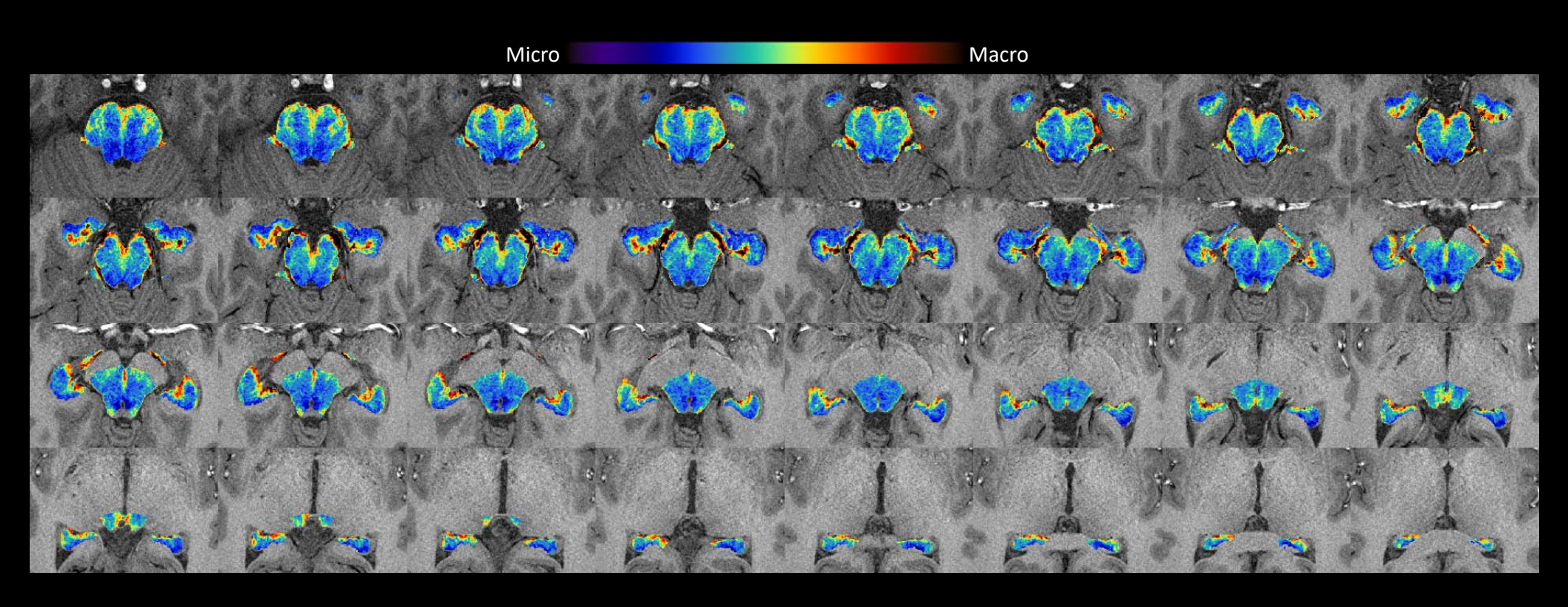


Template of the Cerebral Vasculature



CVS registration: G.M. Postelnicu, L. Zöllei, B. Fischl, IEEE Transactions on Medical Imaging (TMI), Vol 28 (4), April 2009, p. 508-522. L. Zöllei, A. Stevens, K. Huber, S. Kakunoori, B. Fischl, NeuroImage 51 (2010), 206-213

Midbrain-Hippocampal Vasculature



CVS registration: G.M. Postelnicu, L. Zöllei, B. Fischl, IEEE Transactions on Medical Imaging (TMI), Vol 28 (4), April 2009, p. 508-522. L. Zöllei, A. Stevens, K. Huber, S. Kakunoori, B. Fischl, NeuroImage 51 (2010), 206-213

Applications of MICRO Imaging: Multiple Sclerosis

- Multiple Sclerosis (MS) is an inflammatory demyelinating disease
- Etiology of MS is understood to be autoimmune. However, a history exists with growing evidence for disrupted vasculature and flow within the disease pathology
- Multiple pathophysiological events may occur in a vicious circle including:

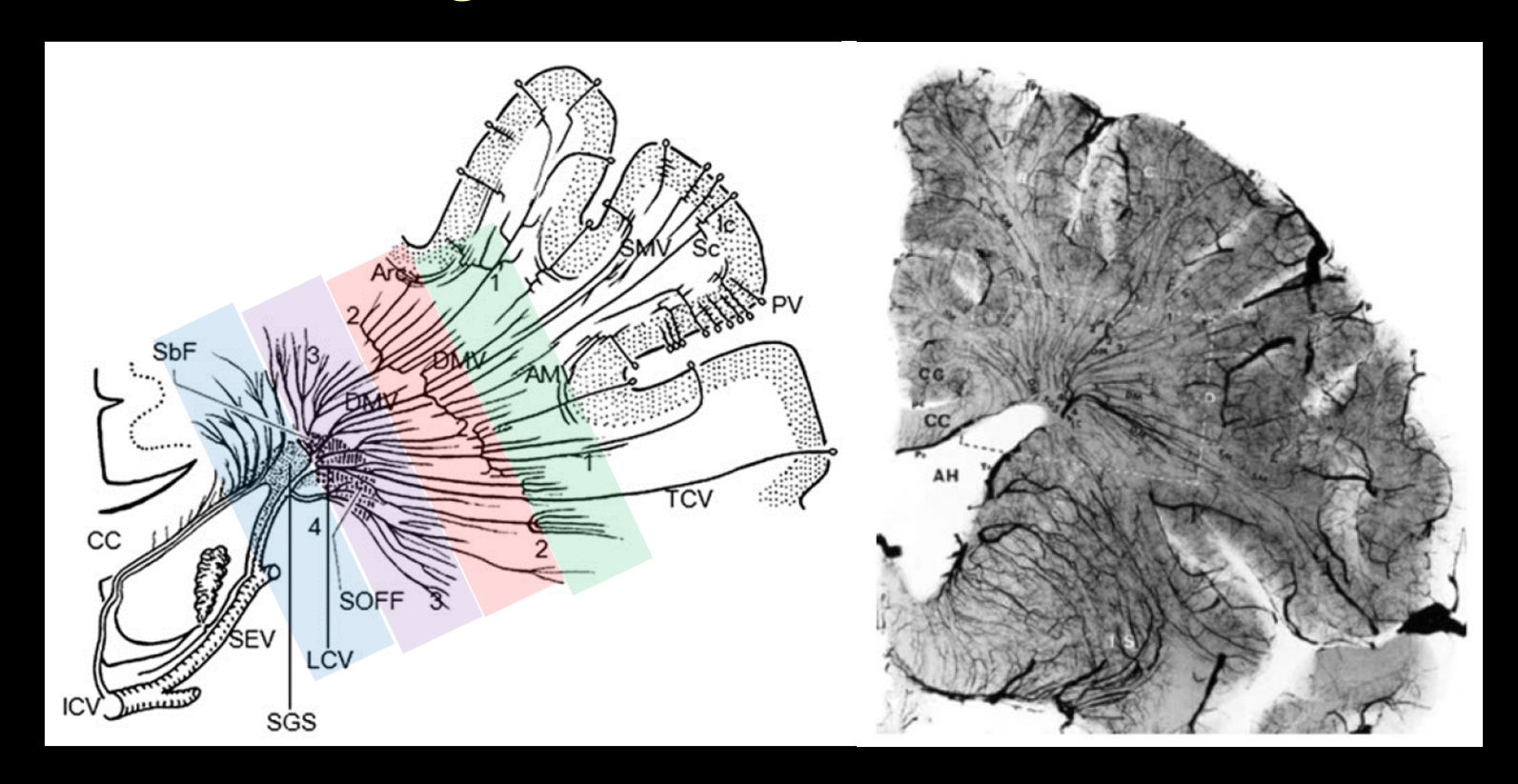
endothelial damage venous collagenosis fibrin deposition

loss of vessel compliance venous hypertension perfusion reduction

medullary vein dilation local vascular remodeling ischemia

 MICRO has potential to monitor the vasculature present in MS lesions and catalogue their characteristics, which may provide new insight into the pathophysiology of MS

Venous angioarchitecture in the cerebrum



1 = first (or outer) zone of convergence

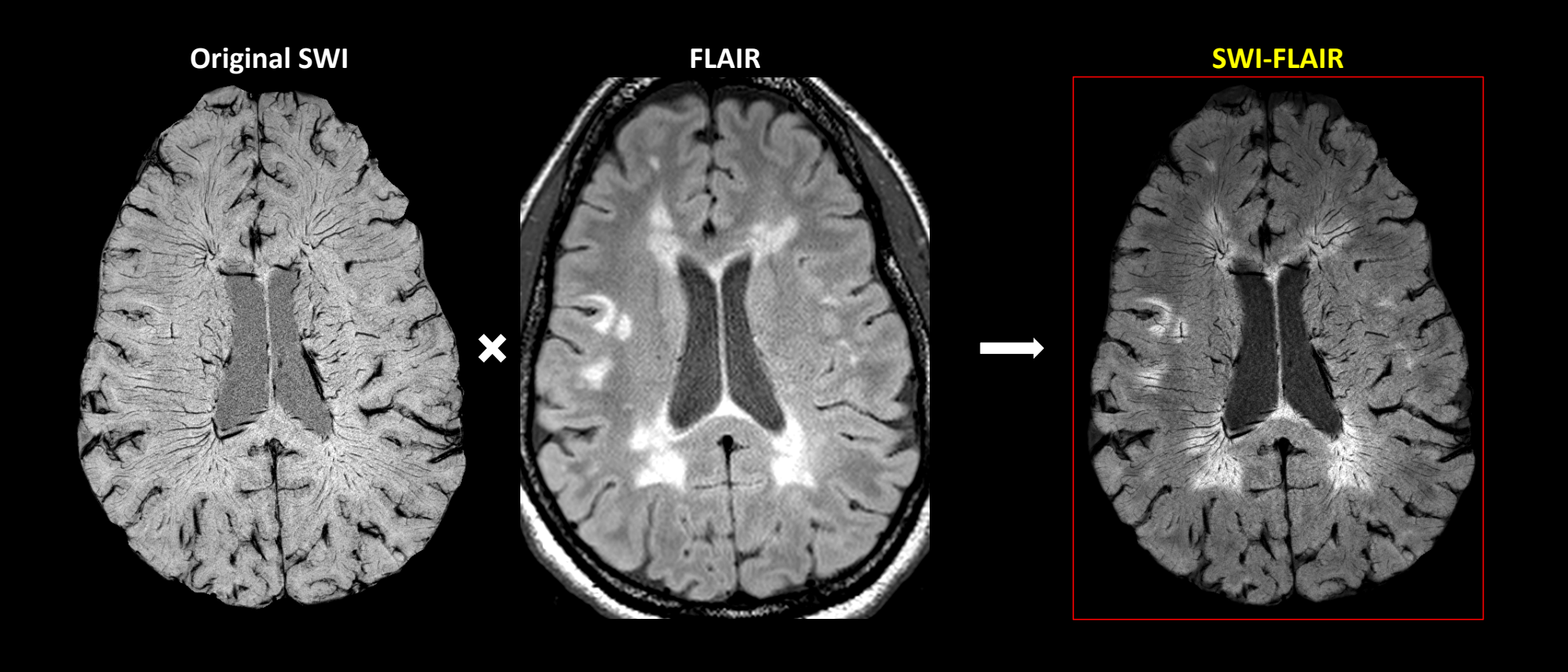
2 = second (or candelabra) zone of convergence

3 = third (or palmate) zone of convergence

4 = fourth (or subependymal) zone of convergence

Taoka, T. (2017). Radiographics, 37, 281.

Generating SWI-FLAIR data



Classifying MS Vascular Anomalies

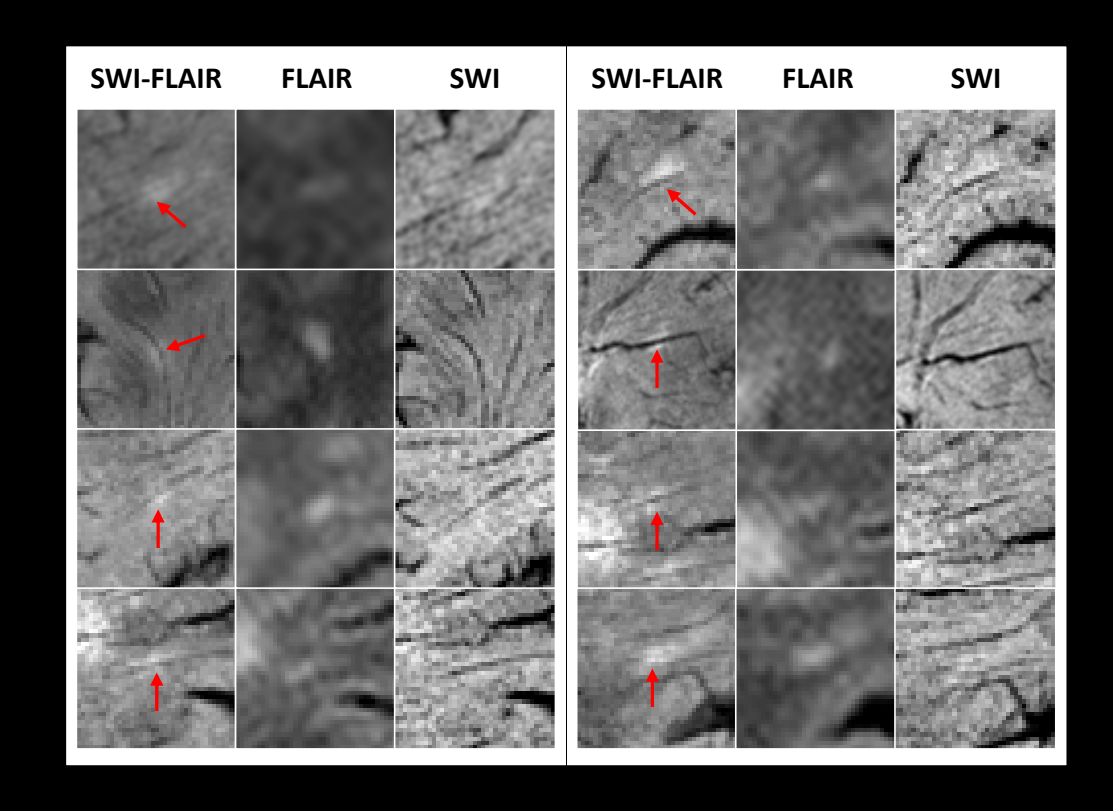
- 1. Small ovoid lesions
- 2. Vessel engorgement (matured collagenosis)
- 3. Perpendicular vessel development (corona radiata)
- 4. Venous angiomas

Small ovoid WMHs

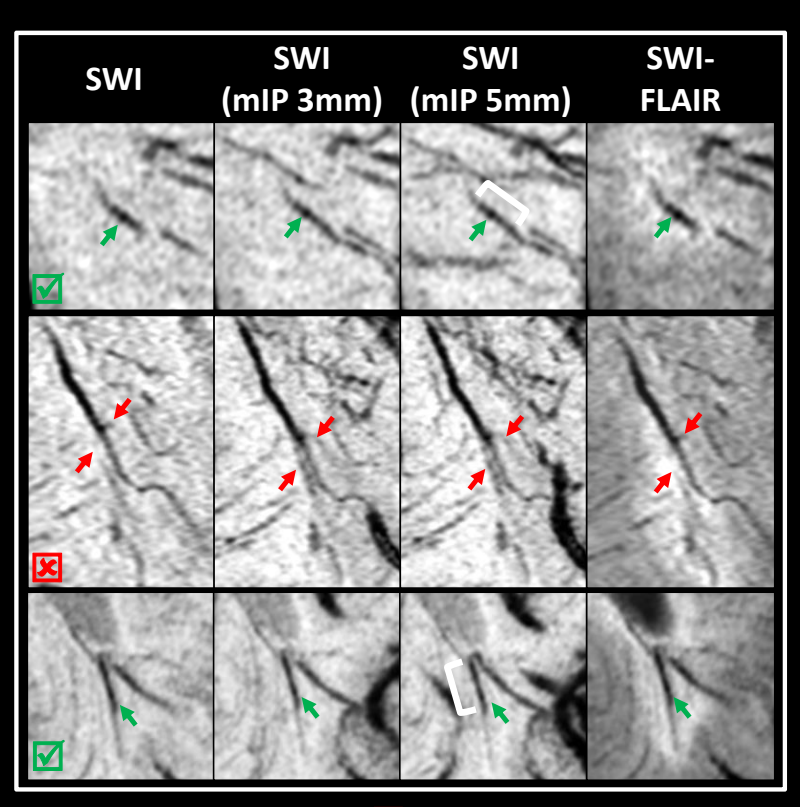
<u>WMH size</u> < 3 mm in-plane and 3 mm through plane



Location of the lesion surrounding a vesse



Dilated vessels show increased intra-lesional diameter with respect to the peri-lesional diameter.

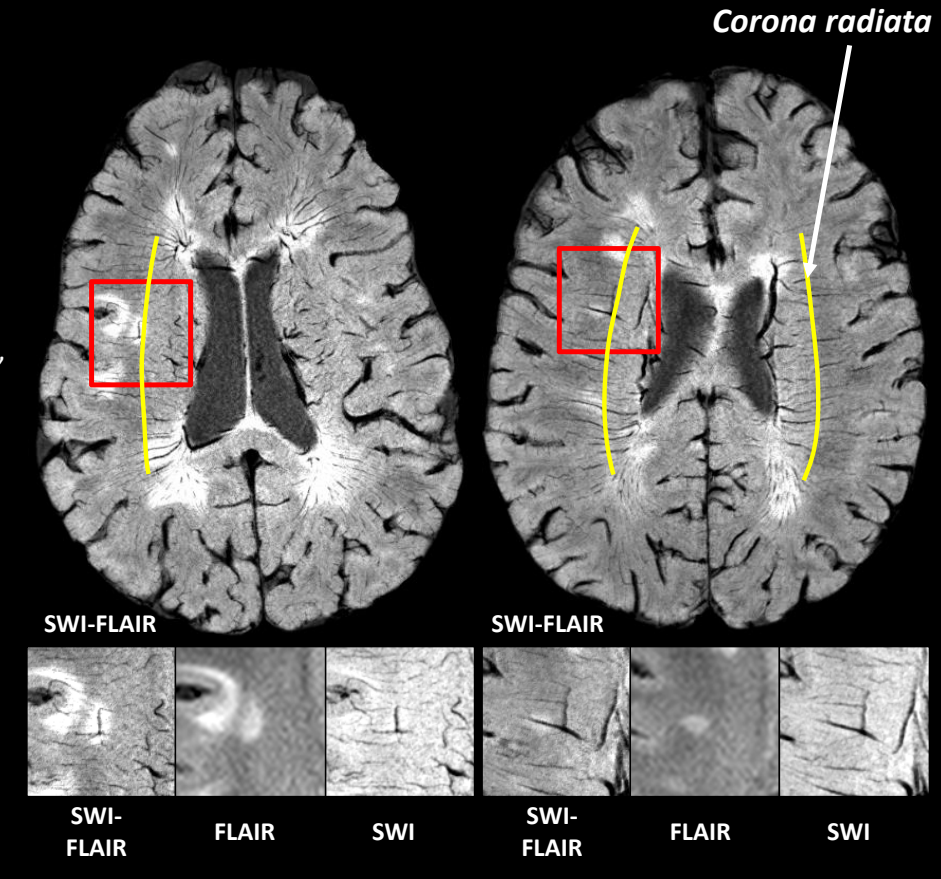


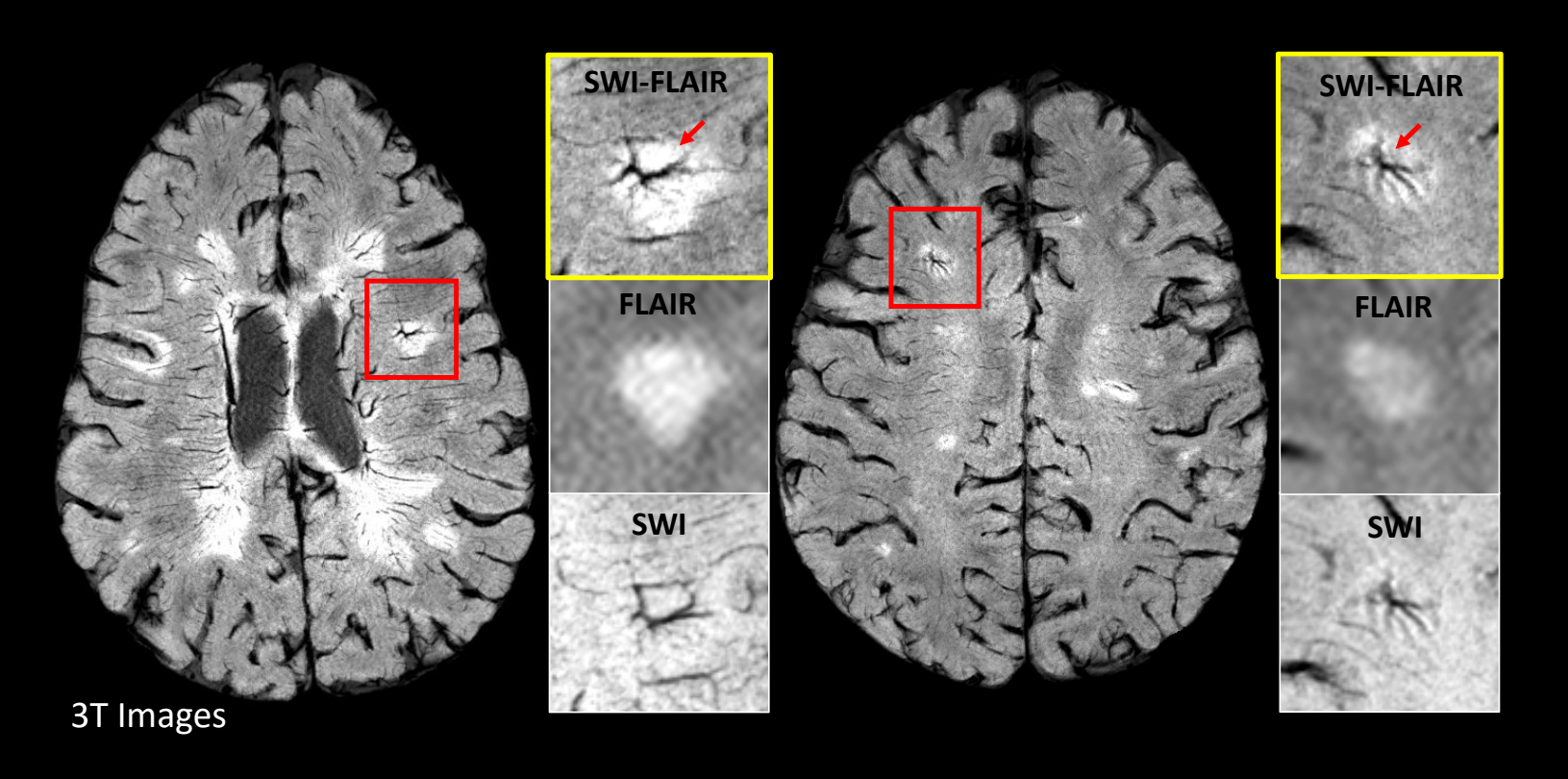
✓ Abnormally dilated vessel

Natural dilation due to confluence

Perpendicular developing vessels

- A perpendicular vessel formation may suggest vascular remodeling (anastomosis), due to local obstructed flow caused by venous collagenosis.
- Usually observed at the boundary of the corona radiata

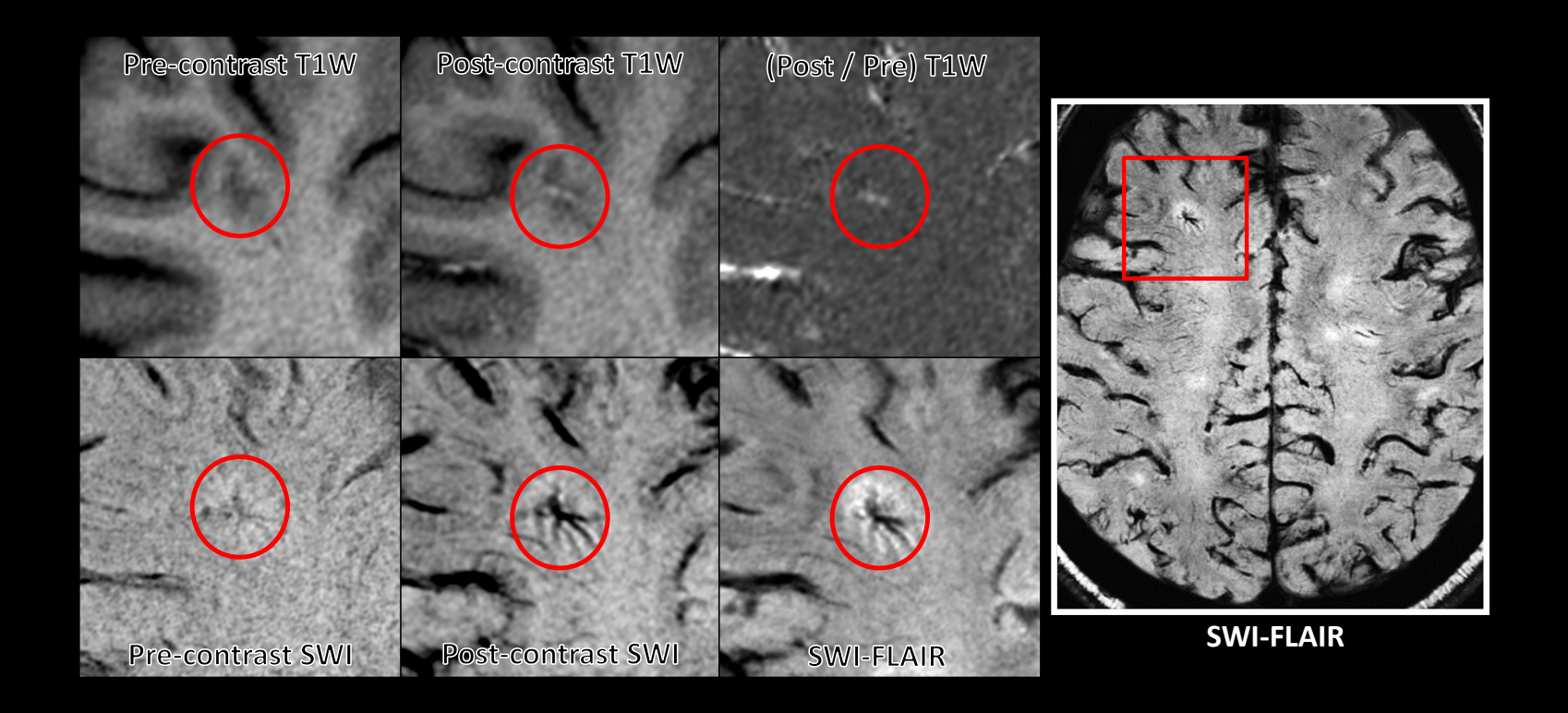




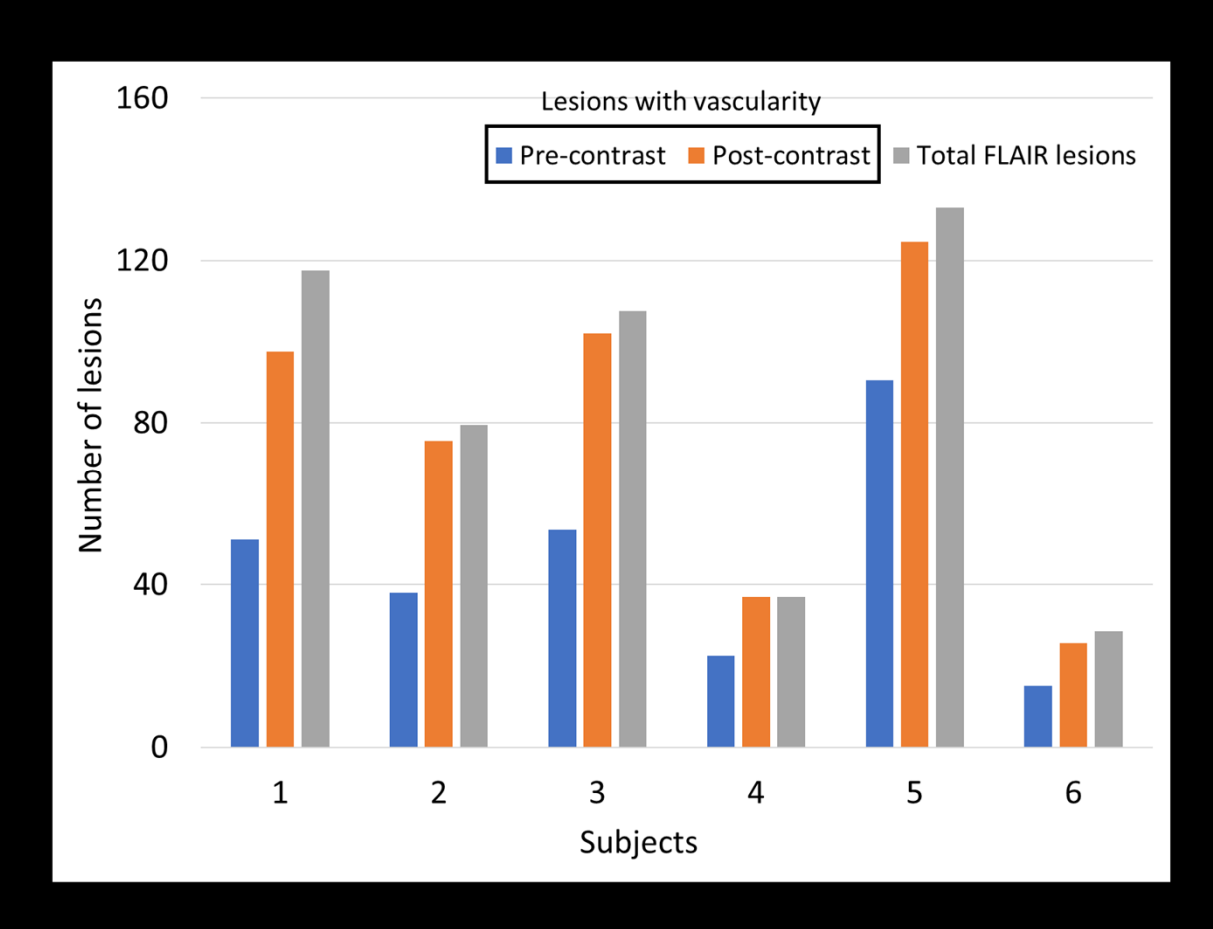
Atypical Venous Angiomas: Cerebro-vascular malformations that involve an irregular arrangement of vessels converging centripetally into a major vessel.

MICRO Imaging:

T₁ enhancement vs T₂* induced signal loss



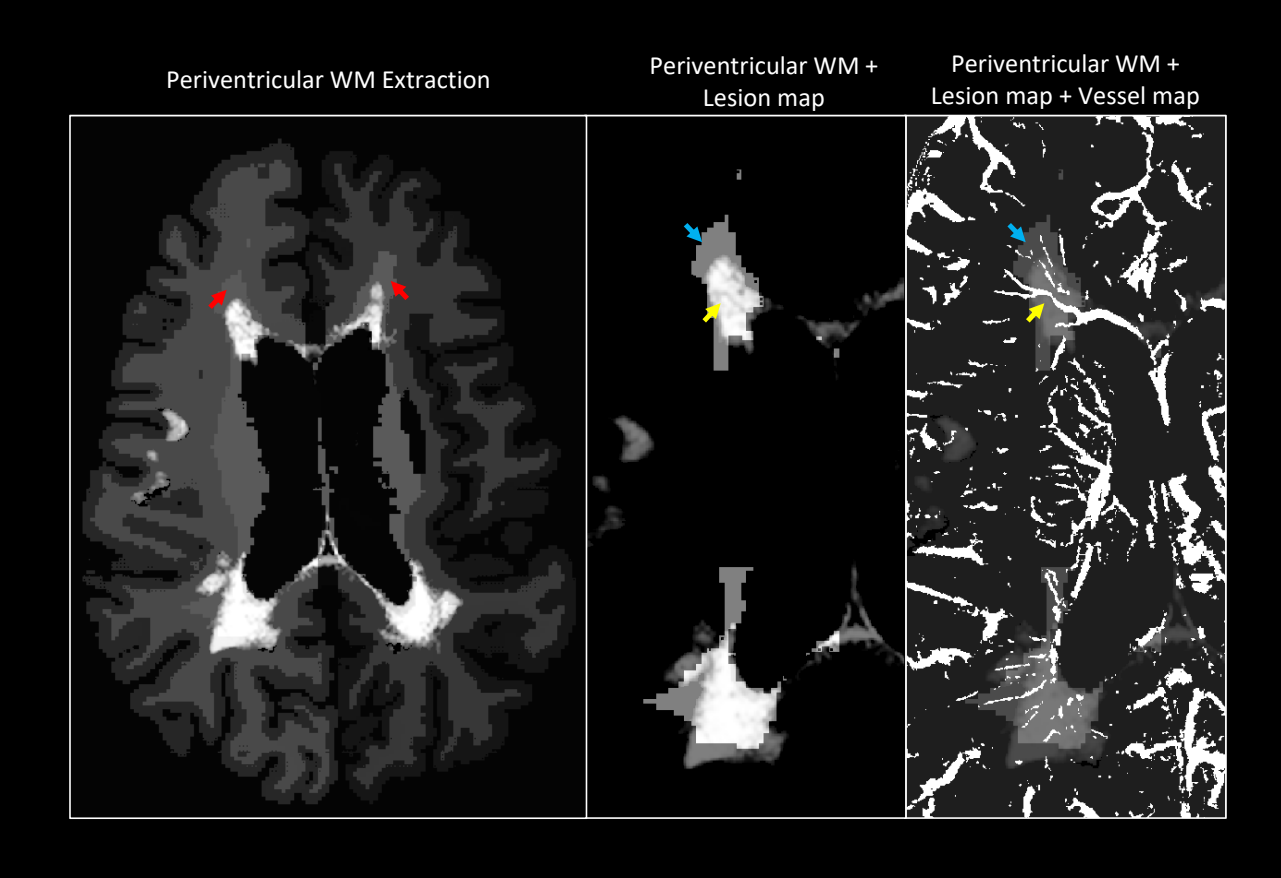
Identifying Vascular Signs in MS lesions



Periventricular WM masks

MICRO Imaging of the Medullary Veins and Multiple Sclerosis

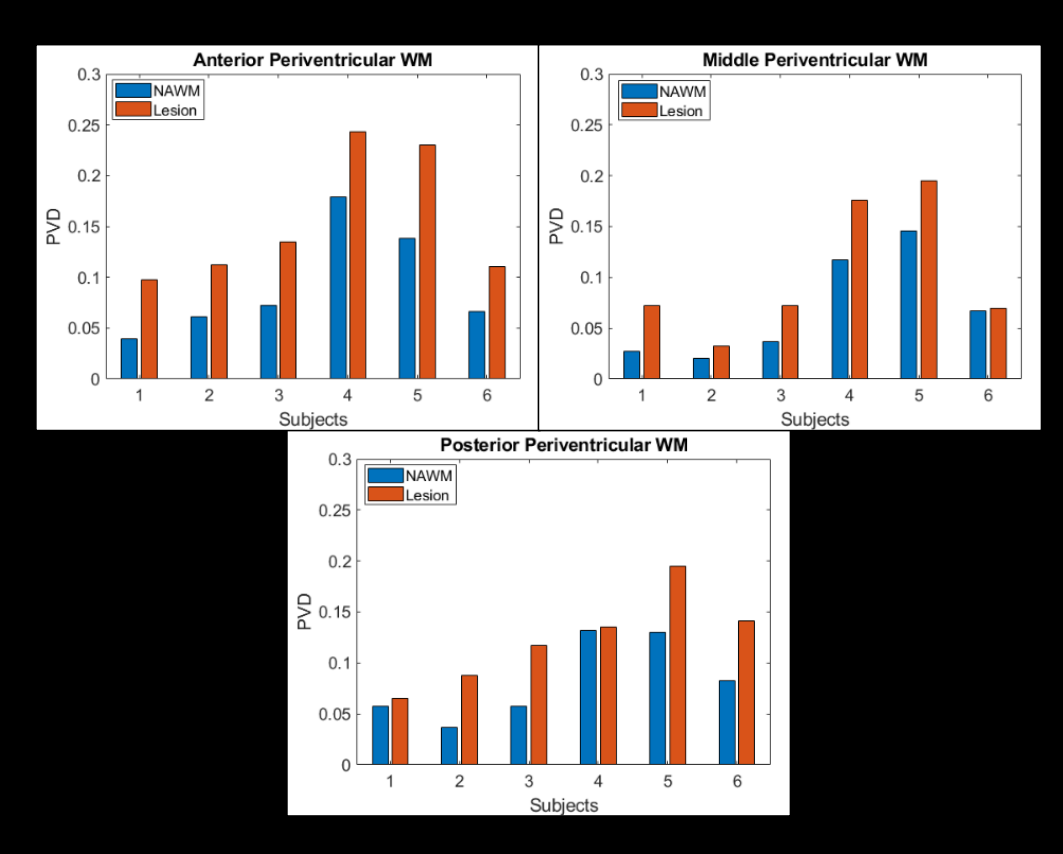




Periventricular WM masks

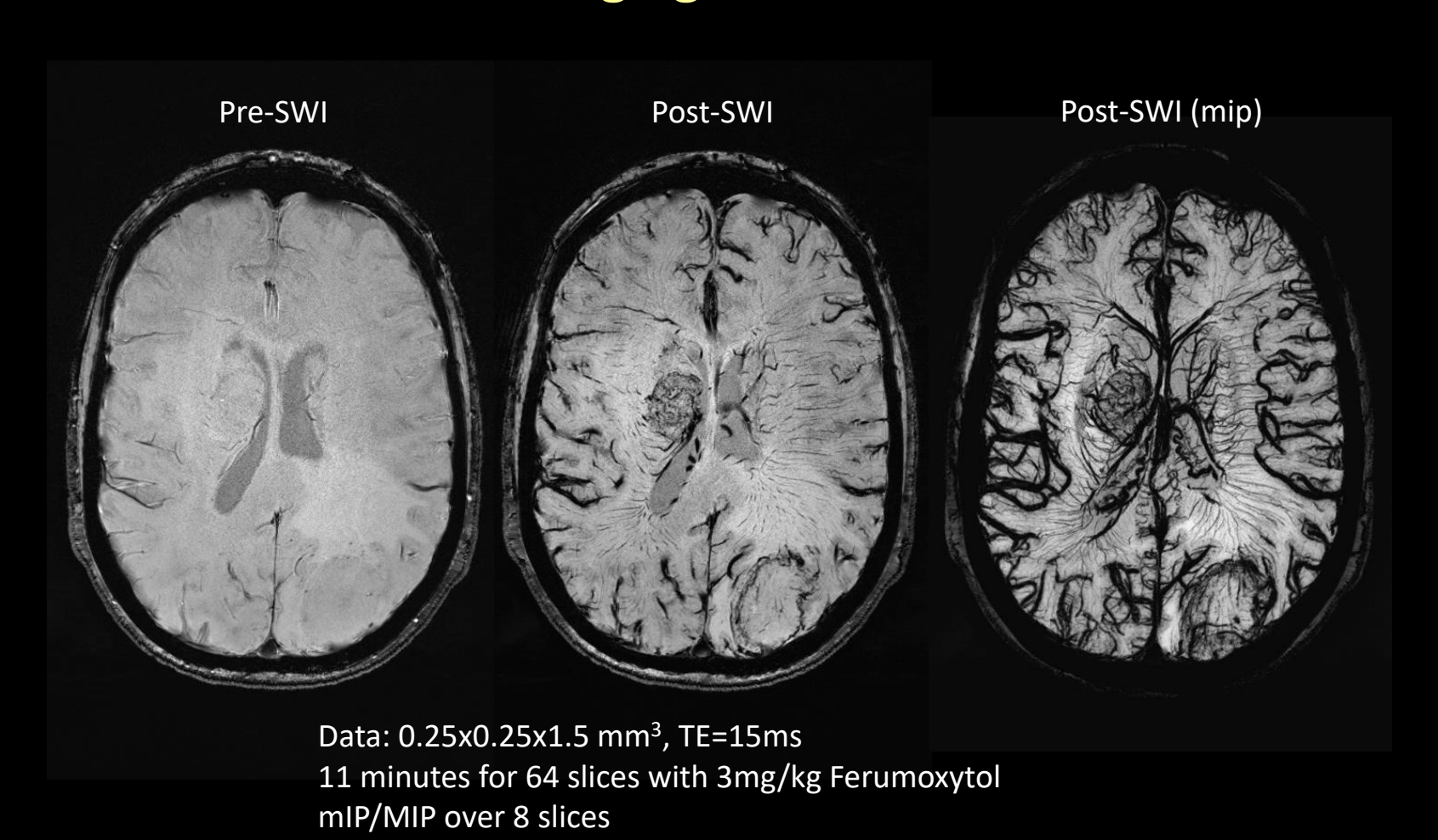
MICRO Imaging of the Medullary Veins and Multiple Sclerosis



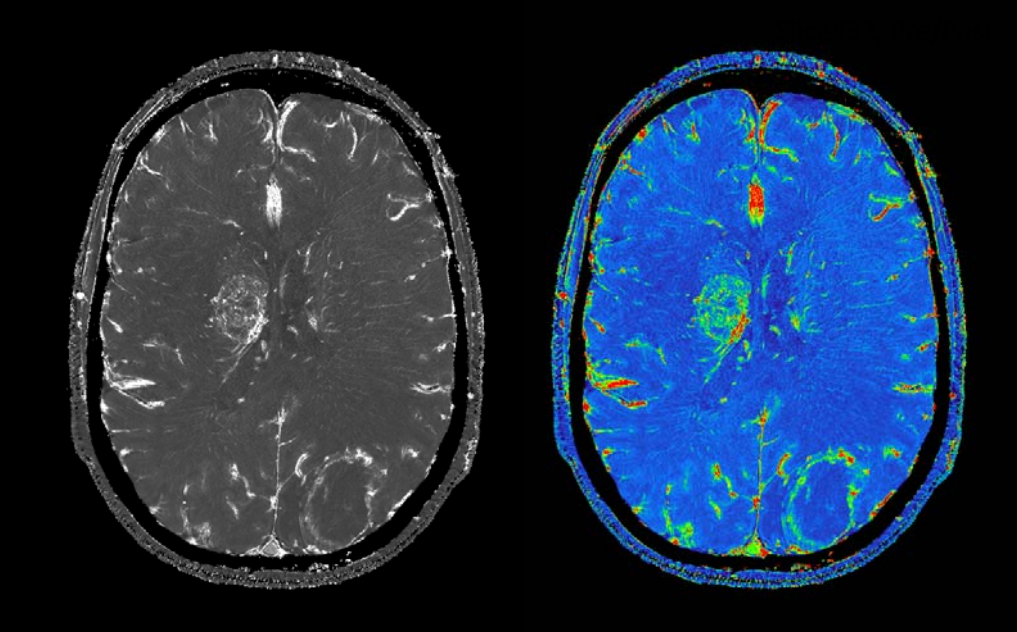


Lesional vessel density is higher than the NAWM vessel density in the periventricular region

MICRO Imaging of Tumors at 3T



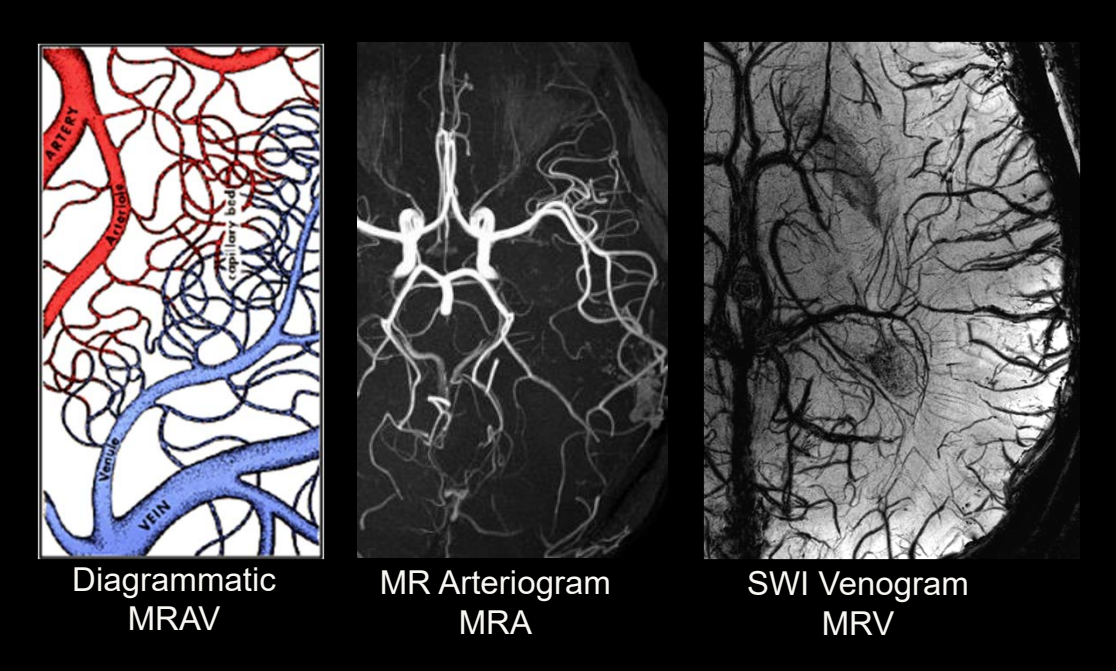
Ratio of pre / post MICRO enhances vascular density



Taking the ratio of pre/post removes all background T_2^* effects and basically gives an R_2^* like map of the vasculature

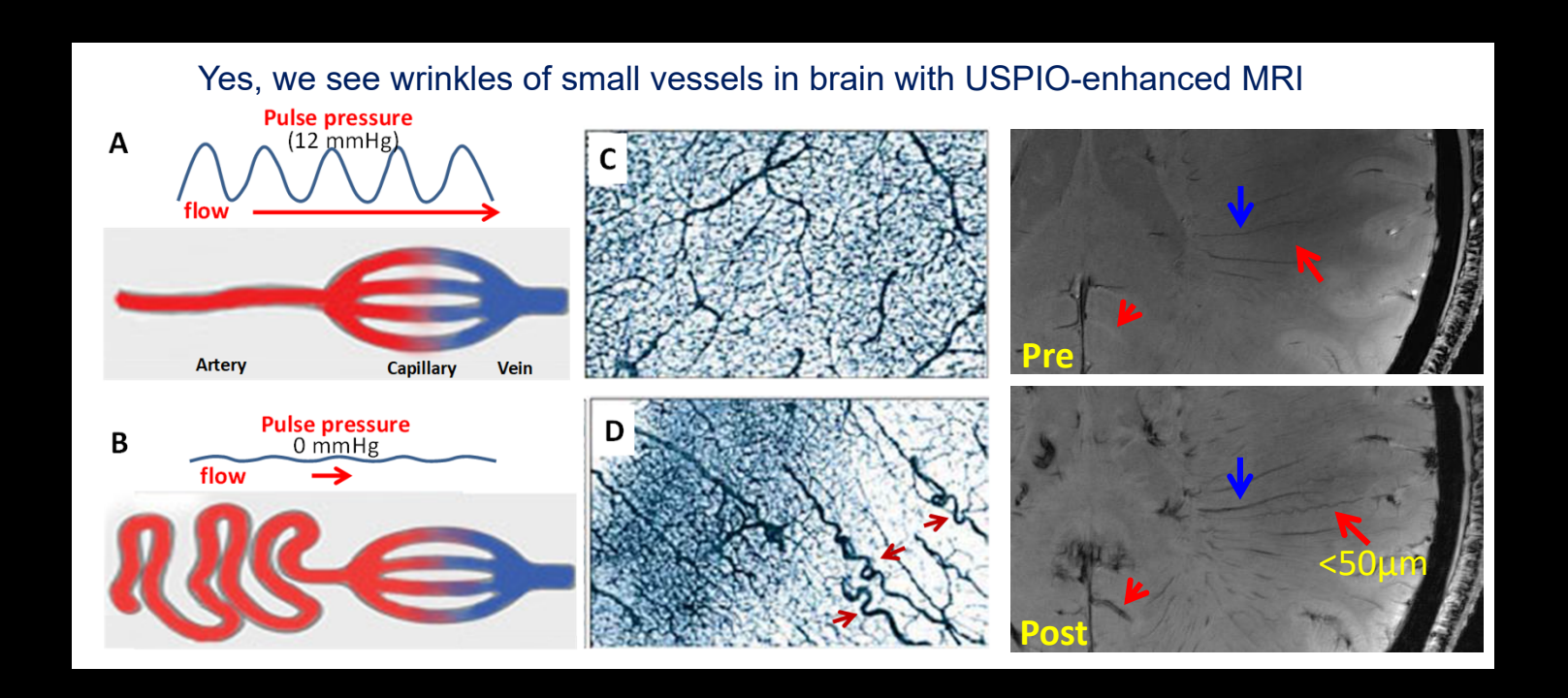
MICRO Imaging of Small Vessel Disease

There is an urgent need to detect damage to small vessels, especially for studying small arteries where vasculogenic neuropathology often begins.



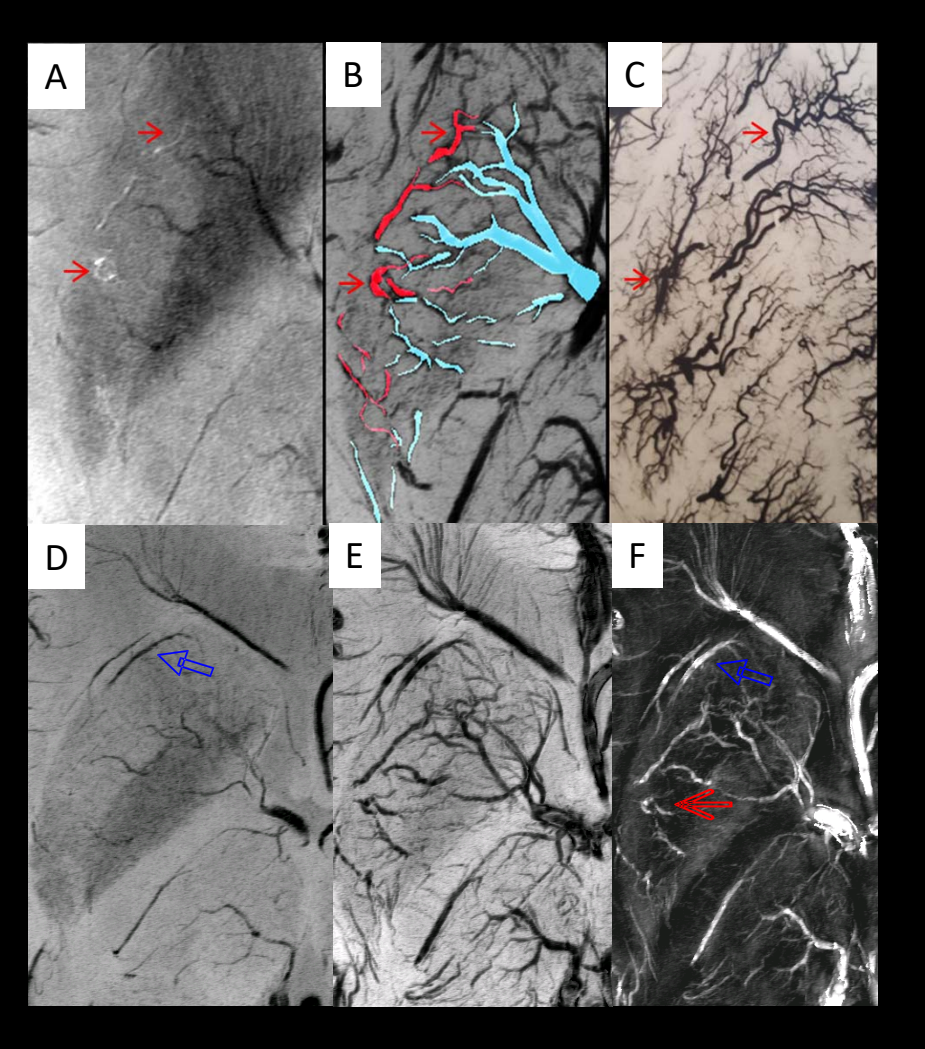
7T Images

Wrinkles in the elderly brain



Part A and B are from Brown WR et al. Review: cerebral microvascular pathology in ageing and neurodegeneration. Neuropathol Appl Neurobiol 2011;37:56-74.

Other Avenues: In vivo MICRO imaging of the Basal Ganglia



7T MICRO data with TE = 8ms and a resolution of $100\mu m$ x $200\mu m$ x 1.25mm.

- (A) MIP pre-contrast magn (arteries in red).
- (B) Post 4mg/kg Ferumoxytol MICRO image.
- (C) Basal ganglia arteries from the cadaver brain work of Georges Salamon (1971).
- (D) mIP of pre-contrast SWI (veins in blue).
- (E) Post-Ferumoxytol SWI (2mg/kg) showing both veins and arteries.
- (F) QSM/SWIM of veins and arteries.

Conclusions

- Imaging the microvasculature of the brain with MICRO is key to unlocking the etiology of many neurodegenerative diseases including: cancer, dementia, multiple sclerosis, stroke and traumatic brain injury
- Imaging with MICRO at 7T offers the potential to image with 250 x 250 x 1000 μ m³ in a reasonable period of time with good SNR
- MICRO imaging brings us into the decade of imaging the microvasculature of the entire human body
- Lesion-pertaining vascular abnormalities were identified using MICRO data with significantly increased detectability